Characterization of Swirling Fluidized Bed

by

Goo Jia Jun

14029

Dissertation submitted in partial fulfillment of
the requirement for the
Bachelor of Engineering (Hons)
(Mechanical Engineering)

MAY 2012

Universiti Teknologi PETRONAS
Bandar Seri Iskandar
31750 Tronoh
Perak Darul Ridzuan

CERTIFICATION OF APPROVAL

Characterization of Swirling Fluidized Bed

by

Goo Jia Jun

A project dissertation submitted to the
Mechnical Engineering Programme
Universiti Teknologi PETRONAS
in partial fulfilment of the requirement for the
BACHELOR OF ENGINEERING (Hons)
(MECHNICAL ENGINEERING)

Approved by,

……………………………
(Chin Yee Sing)

UNIVERSITI TEKNOLOGI PETRONAS
TRONOH, PERAK
May 2012

CERTIFICATION OF ORIGINALITY

I hereby verify that this report was written by **GOO JIA JUN (14029)** and declare that I am responsible for the work submitted in this project, that the original work is my own except as specified in the references and acknowledgements, and that the original work contained herein have not been undertaken or done by unspecified sources or persons.

…………………………………….

(Goo Jia Jun)

ACKNOWLEGEMENTS

First and foremost, the author would like to express a heart filled gratitude to the old Gods for all His blessings that made all things possible throughout the twenty eight weeks of Final Year Project at Universiti Teknologi PETRONAS. The author would also like to express the sincere gratitude and appreciation to all parties for their specific help towards the completion of this research. The author is indebted to following individuals who have contributed to the development of training experiences as well as this final report:

Ms. Chin Yee Sing, *FYP Supervisor*
Assoc. Prof. Dr. Hussain H. Al-Kayiem, *FYP Examiner*
Dr. Aklilu Tesfamichael Baheta, *FYP Examiner*
Prof. Vijay R. Raghavan, *FYP Referee*
Dr. Hasan Fawad Junejo, *FYP Coordinator*
Mr. Vinod Kumar, *Graduate Assistant*
Mr. Mior Rosgiazhar, *Lab Executive*
Mr. Muhamad Hazri, *Lab Technologist*

A particular note of thanks is given to Ms. Chin Yee Sing, for her relentless guidance and never refuses to offer assistance, supports and project ideas throughout the research. The trust placed on the author to carry out the study and consistant devotion of effort and patience to supervise the author will not be forgotten. The author is also grateful to Assoc. Prof. Dr. Hussain H. Al-Kayiem and Dr. Aklilu Tesfamichael Baheta who willing to share irreplaceable and priceless knowledge that they have passed in the project evaluation.

Thus, the time in Universiti Teknologi PETRONAS is very audacious and supportive to the author’s study through which he has gained valuable research experience that will help definitely makes a favourable impression on him as a prospective future employee.

ABSTRACT

This dissertation is intended to conclude and summarize the overall milestone of Final Year Project, Characterization of Swirling Fluidized Bed. In recent years, the Swirling Fluidized Bed has been regarded as one of the novel designs in fluidization technology. This new technique features an annular-blade distributor which injects the fluidizing gas through a certain inclination, is capable of fluidizing the bed and at the same time causes swirling motion of particles in a circular trajectory. In the present work, the fluidization characteristics and hydrodynamics of a swirling bed are studied using experimental approach. The behavior of gas-particle interaction in a swirling bed in terms of operation regimes, trends of pressure drop across particle bed and hysteresis effects of bed pressure drop with increasing superficial velocity of gas, are explored by varying bed configurations. Three different sizes of spherical Polyvinyl chloride particle, two sizes in irregular shape and two sizes in cylindrical form, are used as bed material by considering four bed weights from 500 g to 2000 g, with increment of 500 g in each step, three blade overlap angles of 9°, 15° and 18°, for air superficial velocities up to approximately 3.5 *m/s* and two blade inclination of 10° and 15°. In this report, a well-structured review of the literature is constructed to compile the critical and substantive discoveries in the past researches. Furthermore, detailed research methodology and detailed analysis of experiment results are illustrated and expounded. The findings explicitly show that the solid particle size, shape, and bed weight are the major variables that give significant impact on the fluidized bed characteristics, while the blade dimension has relatively smaller effect on the bed behavior. This project has, hopefully, revealed how everything responds in SFB and this correlated relationship could be a precious benchmark in designing a reactor bed. As a conclusion, the research is intended to demonstrate the superiority of SFB over conventional bed. Through this exploration, the author sincerely hopes that this project will become an achievable reference volume for every practitioner in this field, spanning the boundary of various disciplines especially for fluidization engineering.

TABLE OF CONTENTS

LIST OF FIGURES

LIST OF TABLES

ABBREVIATION AND NOMENCLATURES

θ	Blade angle
d	Diameter
$\frac{L}{D}$	Length to diameter ratio
ρ_g	Gas density
g	Gravitational acceleration constant
μ	Fluid viscosity
ΔP	Pressure drop
U_m	Superficial fluidized velocity
R	Ratio of distributor pressure drop to bed pressure drop
L	Height of bed
G	Mass-flow rate of fluid
D_p	Effective diameter of particles
Ar	Archimedes number
$Re_{p, mf}$	Reynolds number
ε	Fractional void volume
μ_g	Absolute viscosity of fluidizing gas
SFB	Swirling Fluidized Bed
PVC	Polyvinyl chloride
EDM	Electrical Discharge Machining
CNC	Computer Numerical Control
PTV	Particle Tracking Velocimetry

CHAPTER 1

INTRODUCTION

1.1 Background of Study

Fluidization, a process of imparting fluidlike characteristic to a bed of solid particles through suspension in fluid that passes through it, has substantial applications in many industrial operations which involve contact between fluid and solids [1], namely granulation, combustion and gasification of solid fuels, shales or solid wastes, drying of particles, metal surface treatments, regenerative heat exchangers, oxidation or reduction of ores, and catalytic thermal cracking. The conventional fluidized bed has certain downsides such as restriction in gas flow rate to avoid elutriation in bed, limitation on particle size, shapes and magnitude of distribution. Circulating fluidized bed, centrifugal fluidized bed, vibro-fluidized bed, and tapered fluidized bed are the diverse designs that have been employed to overcome some of the limitation of the conventional fluidized bed [2]. One of the recent developments to tackle deficiencies of the conventional bed is the Swirling Fluidized Bed (SFB). This novel variant of the fluidized bed features an annular bed and inclined injection of gas though the distributor blades [3], resulting in a swirling motion of solid particles in a confined circular path. This technique of fluidizing the solid particle bed has a number of unique characteristics, and fluidization engineering is concerned with efforts to take the advantageous behaviors and put them to good use.

Figure 1.1: Swirling fluidized-bed granulation coating machine
Retrieved April 07, 2012 from china-ogpe.

1.2 Problem Statements

Equipment using the swirling bed principle appears to be commercially available for various operations and this new technology has hit the industrial scene in a big way in recent years. Contrariwise, its proud successes do not spur much research efforts, the published information on the characterization of SFB is scanty and in fact there are very few reliable systematic studies of SFB. Arising from extensive literature review, there is still much confusion and contradiction in the reported literature caused by apparent deficiency of credible experimental studies on hydrodynamics characteristics of swirling beds. As a result, the industrial design especially in the reactor application places excessive emphasis on previous practices or on careful scale-up of existing design coupled with liberal sprinkling of safety factors [4]. Consequently, the practice of art governs, technical design from the principle of fluidization characteristic is rarely attempted, and most of the research findings do not seem to be very pertinent in this effort.

1.3 Objectives

This project is aimed to develop a fundamental understanding of the hydrodynamic characteristics of SFB and to attest its superiority over conventional fluidized bed. To explore these properties, detailed experimental studies will be conducted by varying the parameters below:

i. Blades inclination angle (refer to Figure 1.2)
ii. Blades overlap angle (refer to Figure 1.2)
iii. The shape and size of solid particles
iv. The weight of the bed of particles

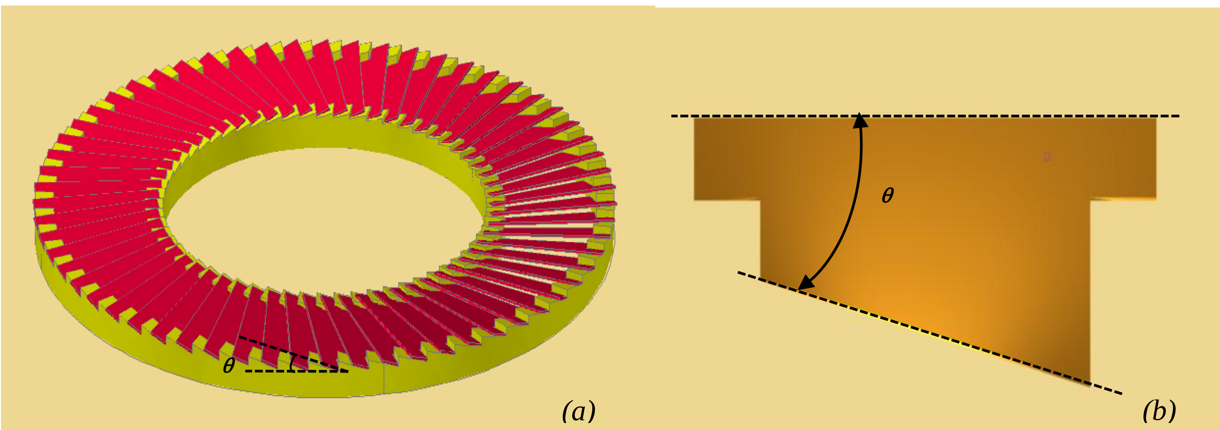

Figure 1.2(a)-(b): Blade inclination angle and blade overlap angle

The hydrodynamic characteristics are comprised of:

i. Pressure drop across the fluidized bed
ii. Hysteresis effect of pressure drop
iii. The flow regimes throughout the fluidization process

In fluidization engineering, these characteristics are fundamental parameters in determining the power required and energy efficiency throughout the process. They also indicate the quality of fluidization and explain the overall hydrodynamic behaviors of the bed. Here the terminology of fluidization quality is defined as the condition of a fluidized bed that possesses an optimal mixing of the gas and the solid particles, with easy handling of bed material, a steady in-bed temperature and mass distribution, and a stable average bed-pressure drop [5].

1.4 Scope of Study

Relatively little has appeared in the open literature related to experiment studies on SFB, the majority of what has been published deals with analytical modeling and other variants of fluidized beds. Therefore, in order to fill the gap of inadequate open references, this project is concerned with hydrodynamic characteristics of fluidization in gas-solid swirling beds; this is a sequel to an earlier work of Jeevaneswary [6]. It is aimed at exploring flow regimes in the beds through visual observation and measurement of bed pressure drops at various flow rates of the gas and at different effects of the parameters mentioned in the Objectives section.

However, the author will not delve into the velocity profile and the motion trajectories of the discrete particles due to time constraint. Furthermore, the formation of 'dead zone' at the center of the bed during operation will not be further investigated. Also, detailed analytical modeling will not be conducted as there are vast literature resources of theoretical studies published by many researchers.

CHAPTER 2

LITERATURE REVIEW

2.1 Fundamental Concepts of Fluidization Process

Various technological operations often necessitate bringing a granular material into intimate contact with a fluid. The simplest way of doing it is through fluidization process, the common concept that is used by different types of fluidization bed discussed in the Background of Study section. Vinod and Raghavan [7], Pigford and Baron [8], Faizal *et al.* [9], and Kunii and Levenspiel [4] observed during the increasing rate of fluid flow upwards through a bed of discrete particles, the pressure drop across the bed will also be increasing until a certain rate of flow, all the particles suspended by the flowing gas or liquid. At this time, the frictional drag force between particle and fluid just counterbalances the particles effective weight and the vertical component of the compressive force between adjacent particles disappears. Subsequently, the pressure drop through any section of the bed about equals the weight of fluid and particles, thus the bed is said to be fluidized (see Figure 3.4). This condition and the velocity of fluid corresponding to it are termed incipient fluidization, and incipient fluidizing velocity (or known as minimum fluidization velocity), respectively. The solid plus fluid becomes as mobile as a true fluid and is called fluidized bed. Indeed, the advantages of utilizing fluidized beds include rapid mixing, resistance to rapid temperature changes and high heat and mass transfer rates [10] [11].

Further increase in fluidizing gas flow rate results in the formation of bubbles or particle-free cavities among the bed particles and this regime is known as bubbling regime. These non-uniformly distributed bubbles rise through the bed, bursting when they reach the free surface, scattering particles into the above-bed region, and lastly fall back to the bed. At this condition, the bed is subjected to fluidization process where vigorous mixing occurs and interaction between gas and particles are intense.

The operation reaches slugging regime when the air cavities are large enough to suspend some portion of the bed weight, giving fluctuation in pressure drop. This undesired regime might not happen for every fluidization process, depending on size of the particle and the type of fluidizing gas. At sufficiently high fluidizing velocity, the particle will become entrained progressively, and the pressure drop will then reduce until, finally, all particles are blown out from the containing vessel [12].

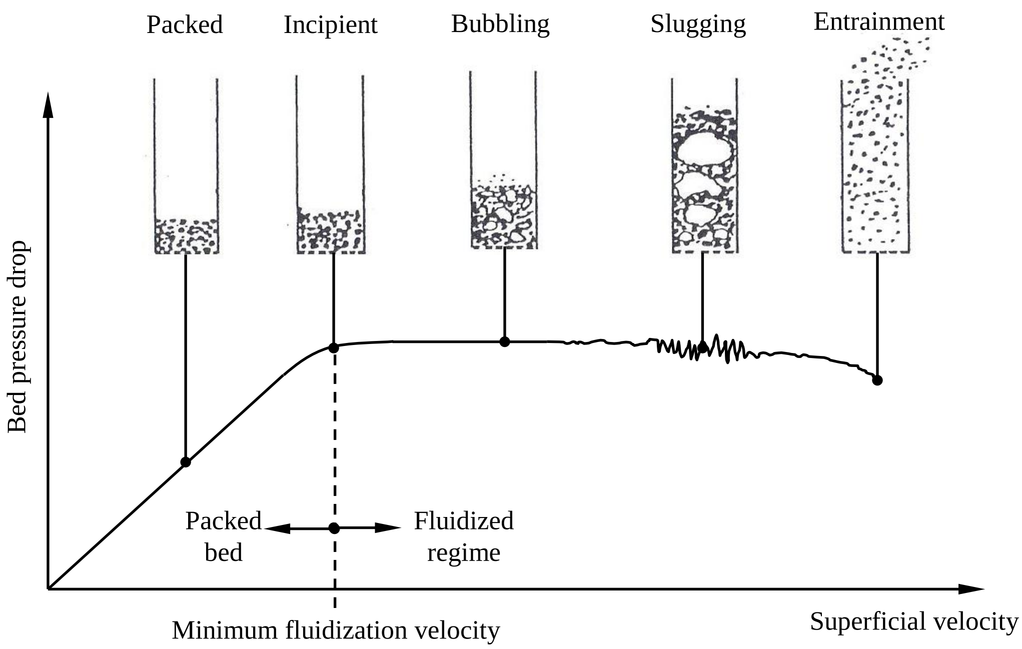

Figure 2.1: Conventional fluidized bed behavior with gas velocity changes

2.2 Swirling Fluidized Bed (SFB)

Sreenivasan and Raghavan [13] had alleged in year 2002 that SFB is the most recent variant in fluidized bed which has set a new benchmark in fluidization engineering. There are plenty of opportunities in this field to be explored in order to improve the SFB as the published information on its characteristic is exiguous. An early work on inclined injection of gas into particle bed was performed by Ouyang and Levenspiel [14] using full width spiral distributor. Their results were perhaps not spectacular to merit further research interest. The change from a full width column to an annular column however renders some remarkable changes in bed behavior. Annular distributor in SFB has the following advantages compared to the conventional bed [9]:

a) Low distributor pressure drop and more energy efficient

b) No bubbling, hence absence of slugging and channeling

c) High quality fluidization with better mixing

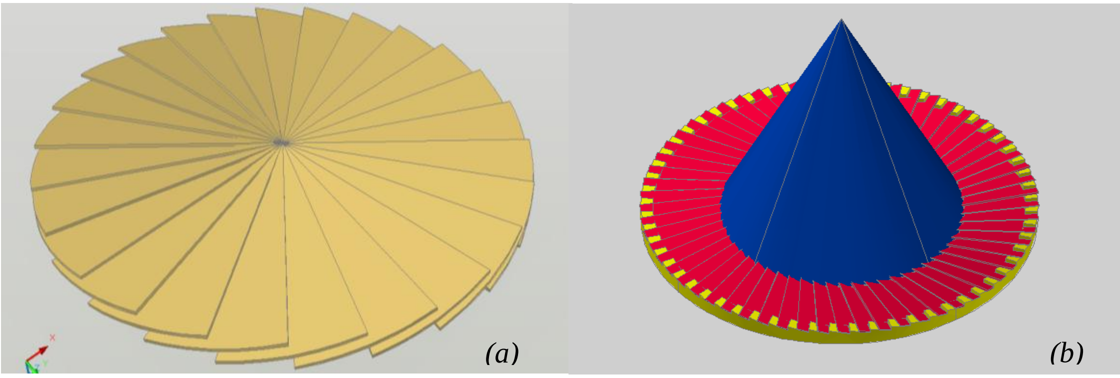

Figure 2.2(a)-(b): Full width spiral distributor design and annular distributor

Another author, Paulose [15] affirmed the superior feature of SFB which is the annular bed, where the injection of gas through the distributor approaches at certain inclination. Therefore, the gas entering the bed will have two components - horizontal and vertical components. The vertical component causes lifting of the particles. It is this lifting force that is responsible for fluidization. The horizontal component, meanwhile, creates a swirling motion force toward the bed particles. Thus, the inclined gas injection fluidizes the bed and at the same time causes swirling motion of particles on confined circular path [16] [17]. The quality of fluidization can be achieved in a SFB with a comparatively lower distributor pressure drop compared to conventional bed. Paulose's theory is then proven by Kaewklum and Kuprianov [18] after conducting experiments using annular distributor with blade inclination that is capable of giving swirl motion to the bed particles.

2.3 Bed behavior of SFB

In present research work, the author measures the pressure drop difference between the tappings P_1 and P_2 (see Figure 3.4). The distributor pressure drop is represented by the pressure drop value for an empty bed and the total pressure drop is denoted by the pressure drop value across a bed of particle. Bed pressure drop is the pressure difference between total pressure drop and distributor pressure drop.

Sobrino *et al.* [19] highlighted the importance of distributor pressure drop which disperses the gas as uniformly as possible over the whole cross-section of the bed. If the pressure drop is very low, the air will enter the bed in the zone of lowest pressure drop and it will cause a non-uniform distribution of air flow inside the bed. Meanwhile, in fluidized bed processes, bed pressure drop is the main element to define the power required for fluidization and justifies the behavior of the flow regime.

S. Ergun [20] has asserted that the pressure drop in a fluidized bed is due to the simultaneous kinetic and viscous energy losses. Ergun's equation, which is established using analytical and experimental approaches, shows the relationship of bed pressure drop with flow rate, properties of the fluids, fractional void volume, orientation, size, shape and surface of the granular solid particles. His equation is as following:

$$\boxed{\frac{\Delta P}{L} g_c = 150 \underbrace{\frac{(1-\epsilon)^2}{\epsilon^3} \frac{\mu U_m}{D_p^{2}}}_{\text{Viscous energy losses}} + 1.75 \underbrace{\frac{(1-\epsilon)}{\epsilon^3} \frac{G U_m^{2}}{D_p}}_{\text{Kinetic energy losses}}}$$

Where by,

ΔP *- Pressure loss*	g_c *- Gravitational Constant*
G *- Mass-flow rate of fluid*	ϵ *- Fractional void volume*
D_p *- Effective diameter of particles*	μ *- Absolute viscosity of fluid*
L *- Height of bed*	U_m *- Superficial fluid velocity*

Paulose [15] expounded the ratio of the distributor pressure drop to the bed pressure drop, R, is generally considered for the design of distributors in conventional bed. Hiby [21], and Geldart and Baeyens [22] claimed that the value of R depends not only on the distributor type but also on the bed particles, the bed depth, the superficial gas velocity, the bed aspect ratio and then percentage of uneven distribution. Only few researchers have come out with R value according to material and type of blade.

Faizal *et al.* [9], Sreenivasan and Raghavan [13] affirmed a striking feature that distinguishes the swirling bed from a conventional fluidized bed is that, the pressure drop of the bed increased with superficial velocity after minimum fluidization in their experimental studies, with the plausible explanation of it is proportional to the bed's centrifugal weight. Faizal and his colleagues also found that the blade geometry has less effect on bed performance, compared to fraction of open area and particle size. Their experiment was aimed to study the effect of the superficial velocity, bed weight, blade overlap angle and number of blades on the bed pressure drop.

Vinod and Raghavan [23] in their research on operation of a swirling fluidized bed quoted that the bed pressure drop first showed an upward trend and upon reaching a particular peak value, it started decreasing. This may be attributed to the fact that the bed pressure drop will fall as the resistance from the bed decreases. Besides, they said that the peak in the bed pressure drop can also be explained as being due to the additional energy required for rearrangement of the 'locked' particles from the packed state in order to get them fluidized. Peng and Fan [24] elucidated the fixed and fluidized regions could coexist in fluidizing bed and give a remarkable pressure drop-flow rate hysteresis loop at incipient fluidization. This theory is supported by a recent work done by Jeevaneswary [5] who claimed on the hysteresis effect on SFB. Besides, experimental study conducted by her has proven that the increasing of bed weight would increase the pressure drop across the bed. She also concluded that spherical particles require higher energy to fluidize followed by elliptical and lastly cylindrical shape. Yet, the effect of overlap angle has not been justified due to the unconvincing experimental results.

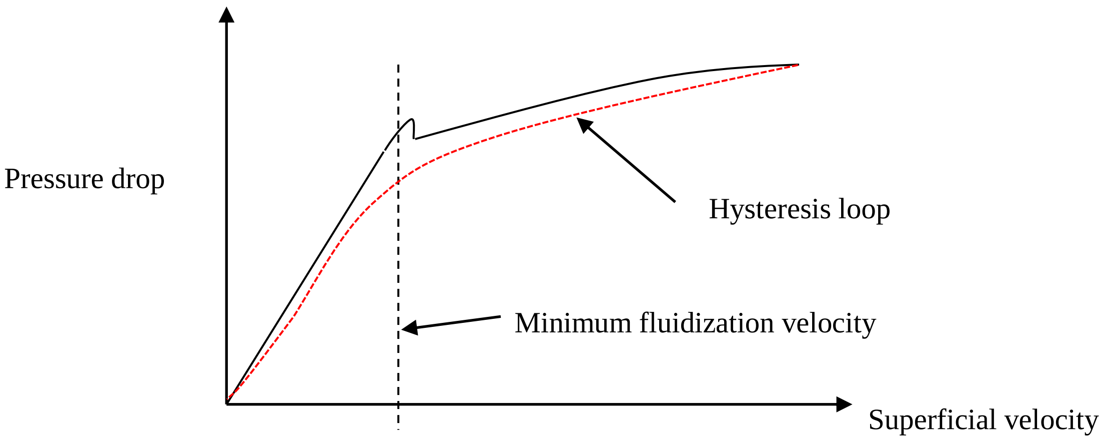

Figure 2.3: Pressure drop profile in SFB

Typical regimes of operation in a conventional fluidized bed include packed bed, minimum fluidization, bubbling, slugging and finally elutriation (see Figure 2.1). While operating a SFB, the following flow regimes occur as the flow rate is increased [13]:

1. Bubbling
2. Wave motion with dune formation: The swirling motion extends over a certain arc of the bed, while the remaining arc is static.
3. Two-layer fluidization: A thin continuously swirling lower layer pairs up with a vigorously bubbling top layer.
4. Stable swirling: Perfect fluidization occurs and the particles swirl smoothly.

Only a few researchers had done research on bed pressure drop. However, their respective research usually will be a part of another research. Therefore, the author gets an advantage since his research is fully on various parameters that influence the characteristics of hydrodynamics during the fluidization of particles.

CHAPTER 3

RESEARCH METHODOLOGY

3.1 Preliminary Study and Conceptual Design

In order to explore hydrodynamic characteristics of fluidization in gas-solid swirling beds, extensive experimental analysis is conducted as a sequel to an earlier work of Jeevaneswary [6]. The set-up is upgraded for a higher range of gas flow rate, more uniform distribution of gas and higher data accuracy. The process of apparatus improvement will be described in the Detailed Design and Actual Apparatus Set Up section. Project Gantt chart, key milestone and activities flow are developed to boil down various timelines and easily comprehend where the author is in a progression.

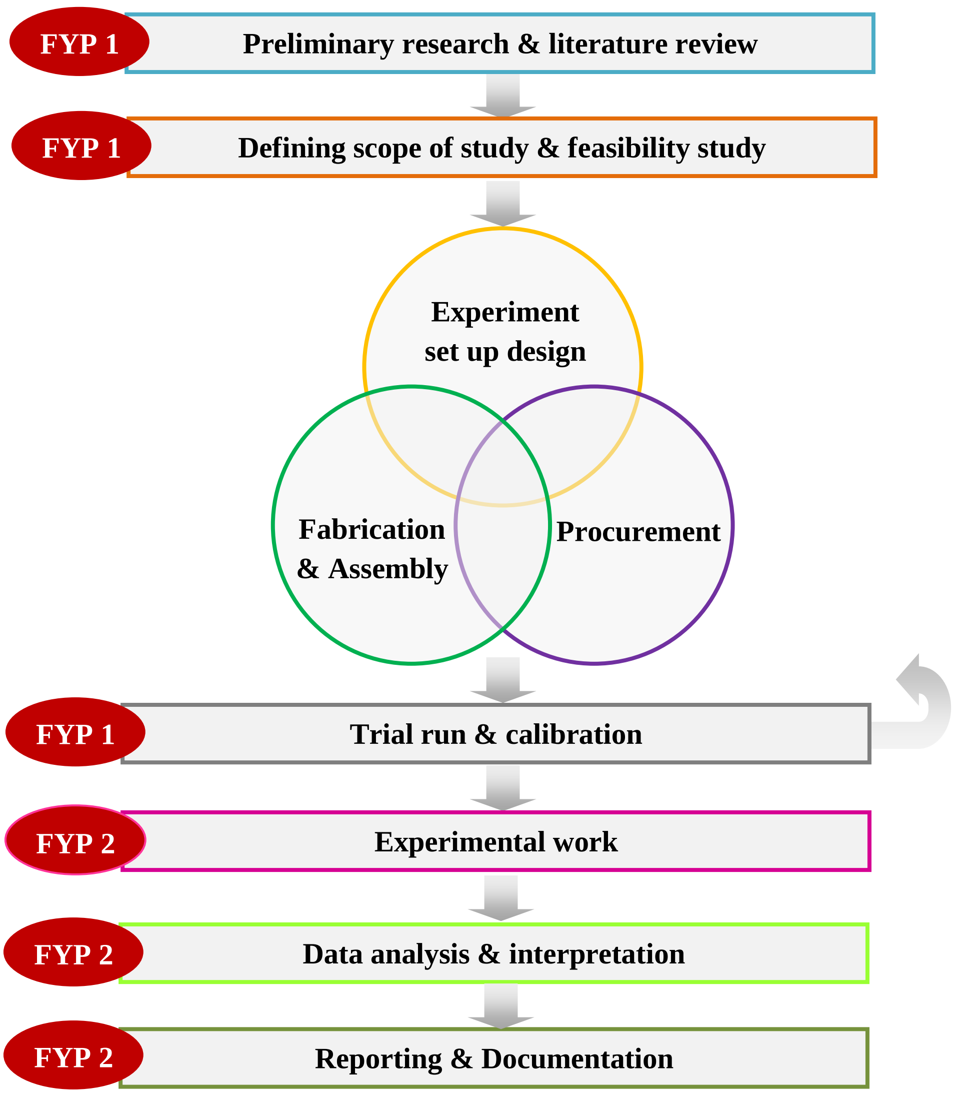

Figure 3.1 : Project activity flow

Table 3.1: Gantt chart and key milestone for FYP 1

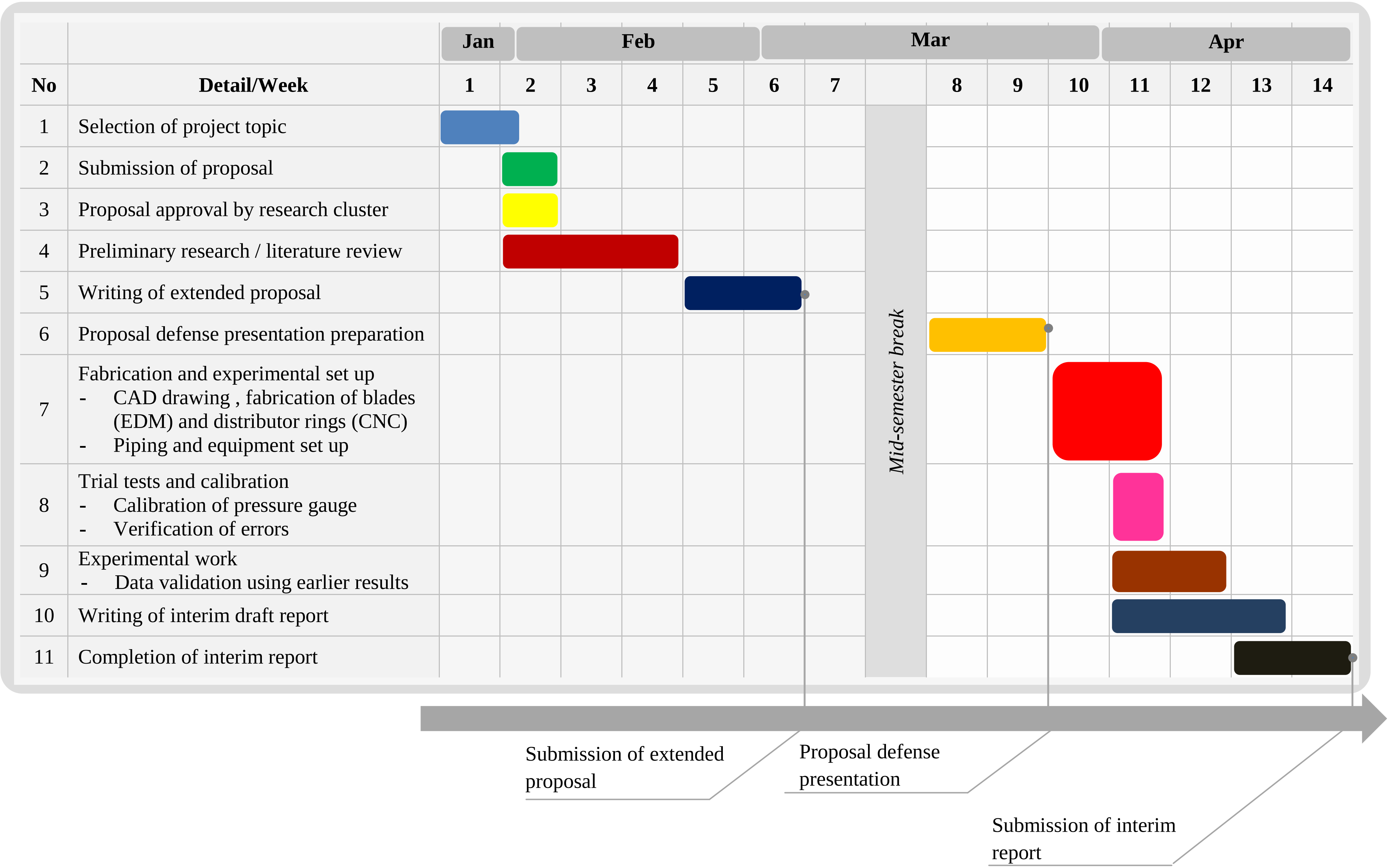

Table 3.2: Gantt chart and key milestone for FYP 2

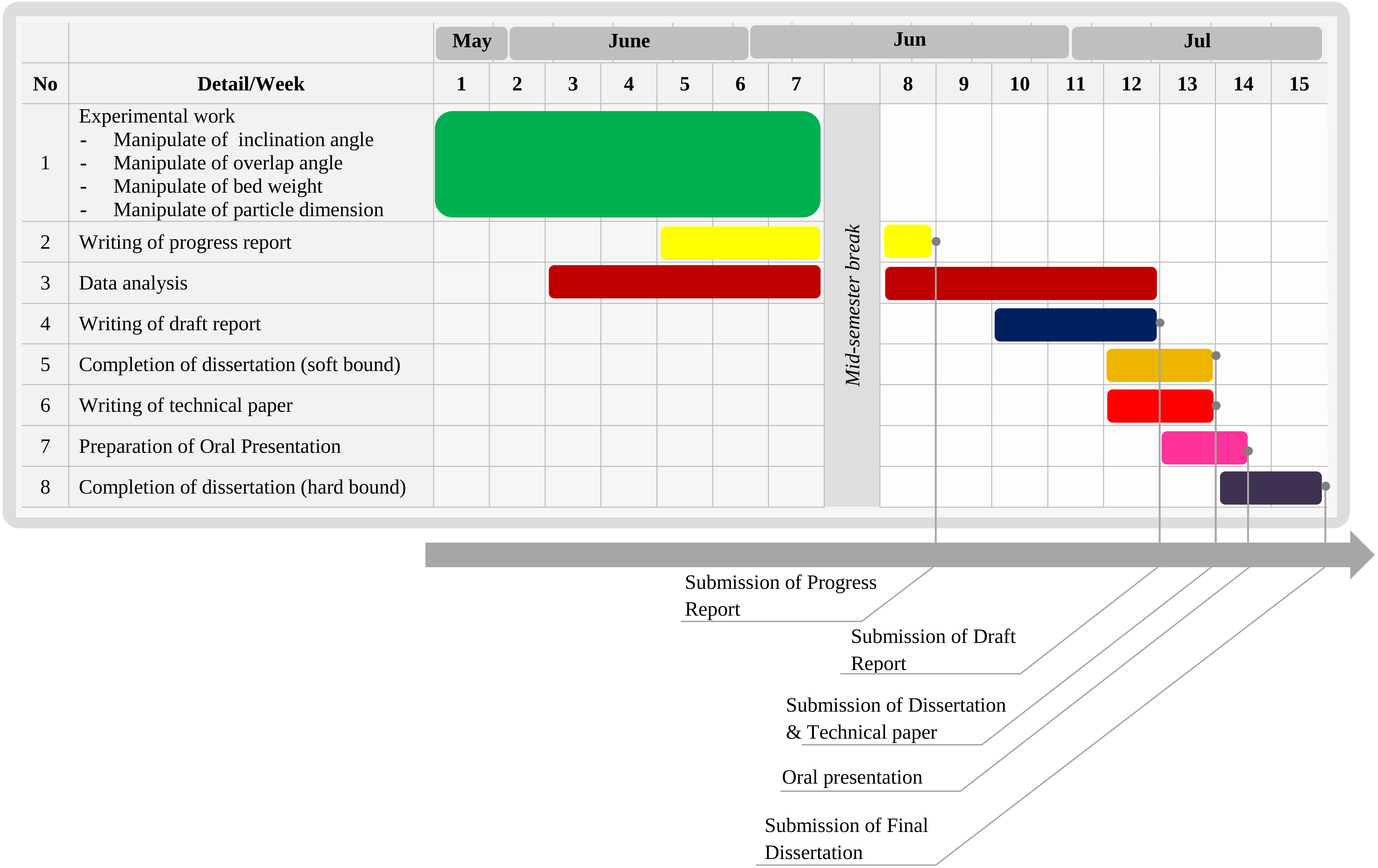

Principally, the apparatus is categorized into 3 segments, namely, input, test bench, and output as illustrated below:

Figure 3.2: Flow schematic for conceptual set up design

In prefatory designs of the experiment set-up, these three major divisions are broke into basic components that must be employed in the experiment in order to create general concept of the arrangement and configuration of the apparatus.

Apparatus		
Input	Test Bench	Output

• Blower
• Piping and fittings
• Weight balance
• Vernier caliper
	• Plenum chamber
	• Distributor
	  - Blades
	  - Blades supports
	  - Cone
	• Pressure tappings
	• Cylindrical bed wall
	• Particles
	• Orifice plate
		• Digital pressure gauge
		• Data recorder

Figure 3.3 : Fundamental division to basic must-have component

The schematic diagram of the conceptual test set-up is shown as following:

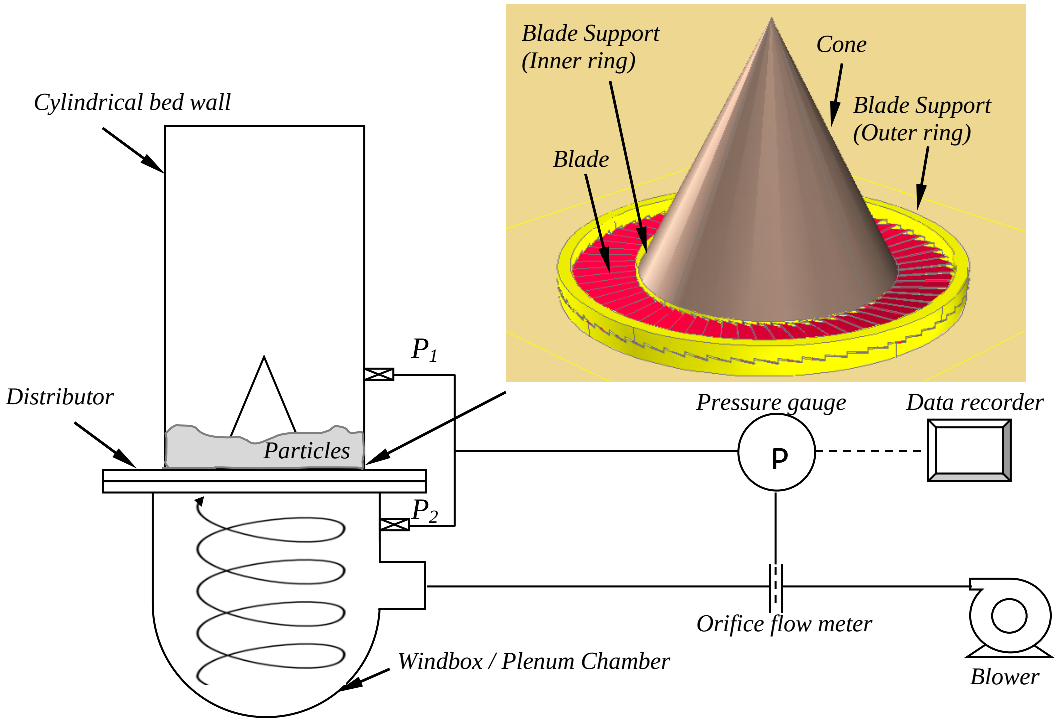

Figure 3.4: Conceptual test set up configuration

3.2 Detailed Design and Actual Apparatus Set Up

This test set-up comprises a Plexiglas cylindrical container acting as a bed wall as shown in Figure 3.5/6 (a). The cylinder is mounted on the flexible version of annular spiral distributor, which is inspired by the spiral distributor design developed by Ouyang and Levenspiel [14]. Unlike them, wherein the overlapping blades formed as full sections of a circle is permanently welded together, the annular distributor is made of sixty blades [3], which are not tack welded at the center (Figure 3.5/6(d)). It features the lightweight and detachable concepts for the ease of varying the configurations with different overlapping and inclination during research work. The inclined overlapping blades help to direct the air at the designed angle. The 1mm-thick aluminium trapezoidal shaped blades are cut by wire electrical discharge machining (EDM) and arranged on Computer Numerical Control (CNC) machined outer and inner stepped rings (Figgure 3.5/6 (c)). The outer rings are supported by a Bakelite block, while the inner rings are placed on a metal hub mounted at the center disk. Both the bed wall and distributor are mounted on the plenum chamber, a hollow cylinder with a hole at one side for the air entry. The chamber is connected to the high pressure centrifugal blower with Polyvinyl chloride pipes, this blower is able to provides higher range of gas flow rate relatively to earlier set up. Air enters the plenum chamber via tangential entry and expands before entering the annular distributor (Figure 3.5/6(b)). This feature results in more uniform distribution of gas compared to set up used by Jeevaneswary [6].

Orifice plates are mounted at middle of the pipe connecting the blower and plenum chamber to quantify the air flow rate. A hollow metal cone is centrally located at the base of the bed. The presence of this cone causes the superficial velocity of the air passes through the distributor to increase, as it reduces the overall cross section of the bed. Hence, this design can operate with relatively deeper beds at high velocity without the problem of particle elutriation. Besides that, it also eliminates the 'dead zone' at the center of the bed. The air flow rate through the bed is obtained by measuring pressure drop across an orifice plate. Two pressure tappings, P_1 and P_2 are provided on the set up, one on the bed wall, the other below the distributor plane, linked to the pressure gauge though pressure fittings and plastic tubes, to measure the pressure drops in mm of water. Each pressure tapping comprises four measuring points located at each quadrant of the cylinders to obtain average or mean value of pressure reading. In the effort to obtain higher data accuracy, data logger is used to record the average value of pressure readings for certain period of time. The snapshot of overall equipment setup is shown in Figure 3.7, the details and dimensions are illustrated in Figure 3.8. A total of seven types of particles with different dimensions are used in the experiment, as tabulated in Figure 3.9.

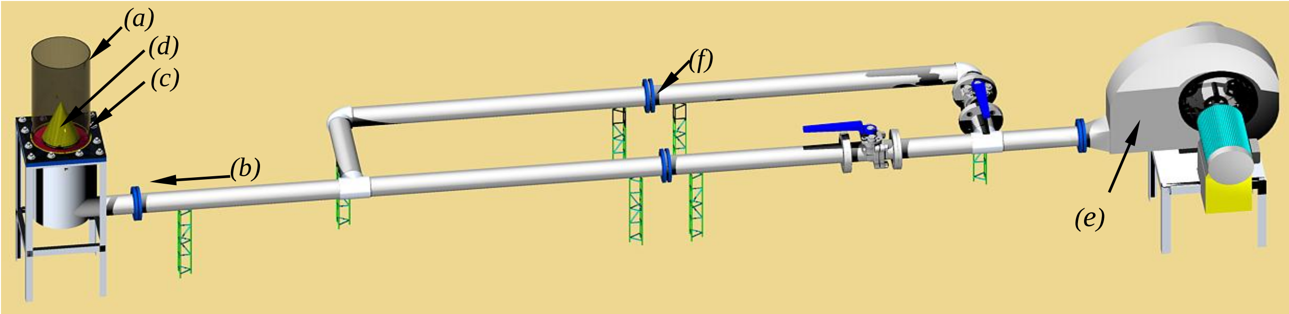

Figure 3.5: Computer aided design of apparatus set up

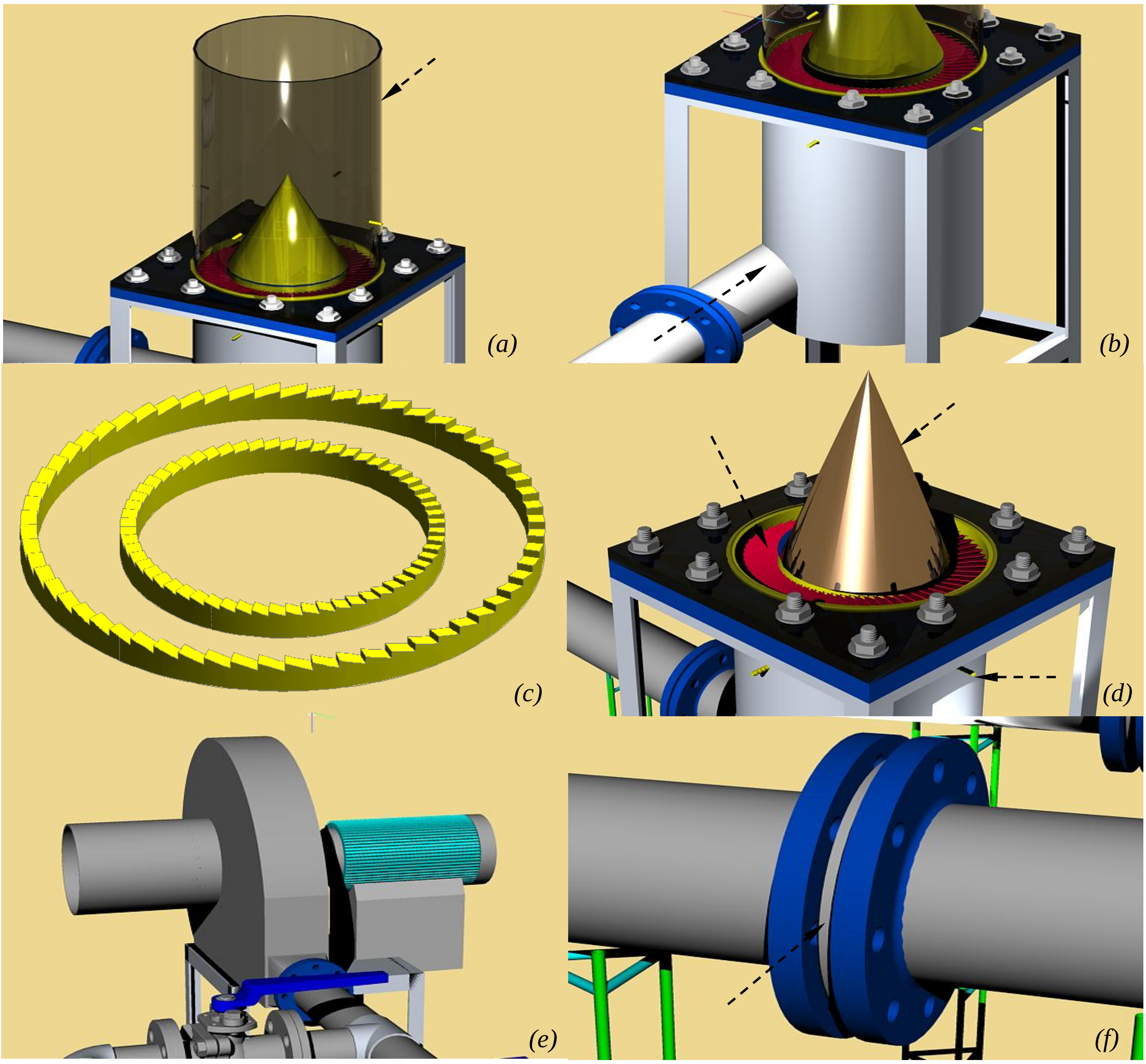

Figure 3.6 (a)-(f): Components of the apparatus set up: (a) cylinder Perspex mounted on top of distributorplane, (b) tangential air entry into plenum chamber, (c) inner & outer blade support rings, (d) distributor, cone & pressure tapping positions, (e) high pressure centrifugal blower, (f) orifice plate

Figure 3.7: Actual apparatus set up

3.3 Tools Dimension and Specification

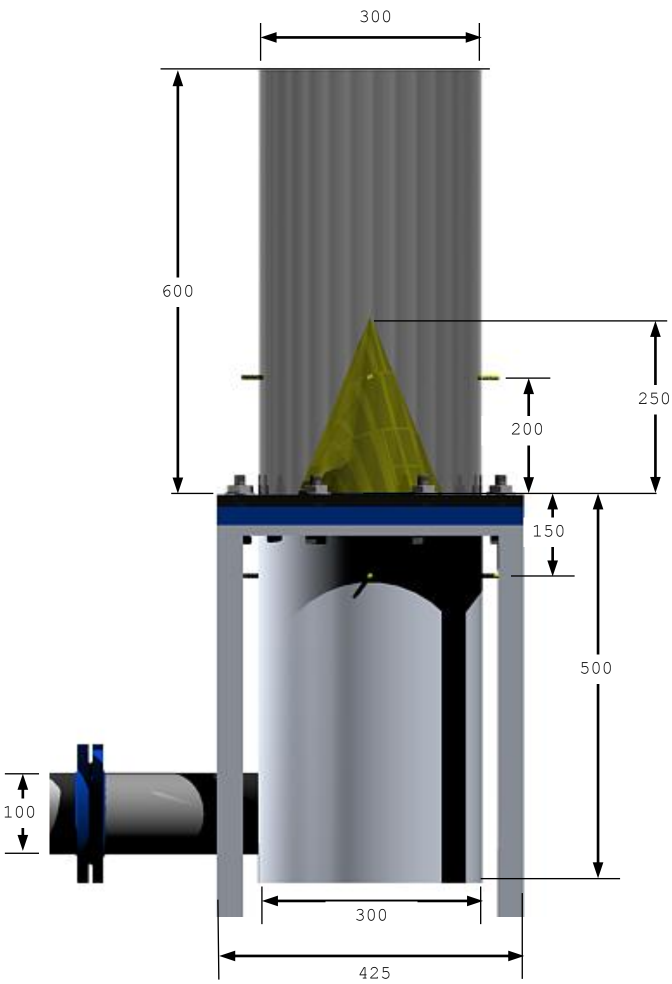

Figure 3.8: Fluidized bed dimension (in unit of mm)

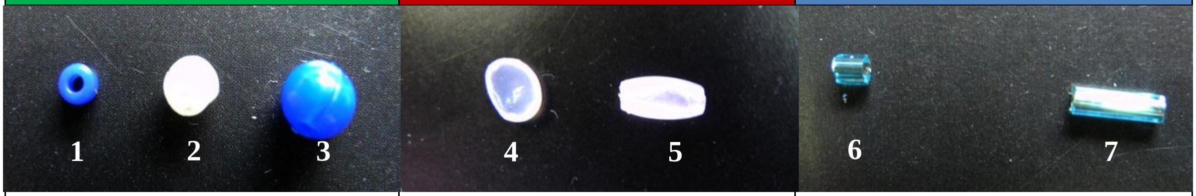

Spherical	Irregular	Cylindrical
$d_1 = 1.20mm$ $d_2 = 2.70mm$ $d_3 = 3.90mm$	$\left(\frac{L}{D}\right)_4 = 1.36$ $\left(\frac{L}{D}\right)_5 = 2.00$	$\left(\frac{L}{D}\right)_6 = 1.28$ $\left(\frac{L}{D}\right)_7 = 4.10$

Figure 3.9: Particle shapes and dimensions

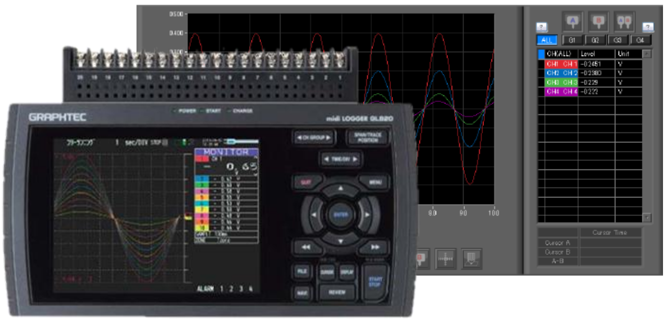

Model	GRAPHTEC midi logger GL820
Software version	GL220_820APS

Figure 3.10: Data recorder and software version

Calculation of orifice flow meter

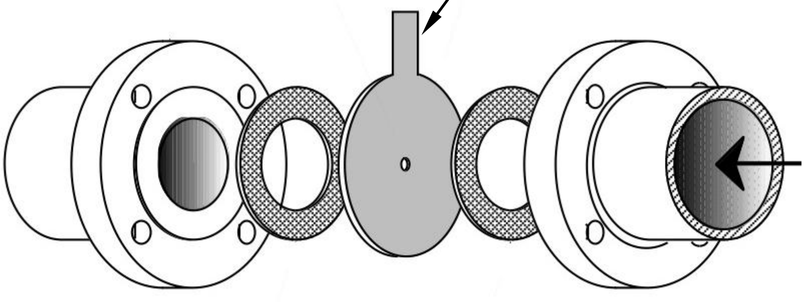

Figure 3.11: Flow through an orifice plate

$$\text{Superficial Velocity, } V_{\text{superficial}} = \frac{\text{Fluiziding air flow rate, Q}}{\text{Bed area, } A_{bed}}$$

Fluidizing air flow rate, Q

$$= \text{Orifice plate area, } A_o \times \text{Coefficient of discharge, } C_d \times \sqrt{\frac{2 \times g \times \left(\frac{\text{Pressure difference, } \Delta P}{\text{Air density, } \rho_{air}}\right)}{1-(\text{Beta ratio, } \beta)^4}}$$

Whereby,

Pipe diameter, D = 0.1 m

Orifice diameter hole, d = 0.062 m

Coefficient of discharge, $C_d = 0.668$

Air density, $\rho_{air} = 1.2 \text{ kg/m}^3$

Beta ratio, $\beta = \frac{d}{D} = \frac{0.062}{0.1} = 0.62$

Orifice plate area, $A_o = \frac{\pi \times d^2}{4} = \frac{\pi \times 0.062^2}{4} = 0.003019 \text{m}^2$

Bed area = $\frac{\pi}{4}\left(\text{Bed outer diameter, } d_o{}^2 - \text{Bed inner diameter,} d_i{}^2\right) = \frac{\pi}{4}\left(0.3^2 - 0.2^2\right) = 0.03927\ m^2$

Thus,

$$\text{Superficial Velocity, } V_{\text{superficial}} = \frac{0.003019 \times 0.668 \times \sqrt{\frac{2 \times 9.81 \times \left(\frac{\text{Pressure difference, } \Delta P}{1.2}\right)}{1-0.62^4}}}{0.03927}$$

$$= 0.2249\sqrt{\text{Pressure difference, } \Delta P}$$

3.4 Experiment Procedures

1. Blades of overlap angle 9˚ are arranged on the 10˚ inner stepped ring at Bakelite and the 10˚ outer stepped ring is placed on the blades to keep the blades in place.
2. The thin carbon steel disk of 5 mm thick is screwed at the center of the bed above the stepped rings in order to keep the blades in place tightly.
3. Then, the central cone is screwed at the center of the bed.
4. Next, the Perspex cylinder is screwed with bolts and nuts to the plenum chamber.
5. The experiment set up is tested with the blower switched on to confirm the experiment set up works well without any failure or leakage.
6. Blower is switched on again.
7. Then, the distributor pressure drop is measured at different air flow rates.
8. The air flow rate is varied progressively using electronic speed controller of blower.
9. The air flow rate is measured using an orifice flow meter.
10. The bed is loaded with 500 g cylindrical particle.
11. The total pressure drop across the bed and distributor is measured for different air flow rate.
12. Then, the experiment is continued with 1000 g and 1500 g and 2000 g of cylindrical particle.
13. The experiment is repeated for blade overlap angles of 15˚ and 18˚ with six others particles shapes.
14. All procedures are repeated using 15 ˚ of blade inclination angle.

CHAPTER 4

RESULTS AND DISCUSSIONS

4.1 Operation Regimes

The operation regimes of a conventional fluidized bed throughout the fluidization process consist of packed bed, incipient fluidization, bubbling, slugging and lastly elutriation. Since this paper does not study the bed pressure drop during packed bed regime, the trend is therefore represented with a dotted straight line. However, the pressure drop curve is predicted to be linear initially, and then it might curve upwards to reflect the higher resistance of a turbulent flow of gas through the particle interstices. In operating a SFB, the author observed that it has distinctive regimes of operations when operating a comparatively shallow bed and deep bed. In packed bed regime, the shallow bed has height range of 5 mm to 20 mm while in relatively deep bed, its height ranges between 35 mm to 45 mm. In the relatively shallow bed (Figure 4.1), with the increase of fluidizing gas superficial velocity, packed bed regime occurs before the incipient fluidization. The incipient fluidized regime is the minimum fluidization condition before the bed is led to swirling condition. Some particles are even started to agitate (minor bubbling) and about to swirl at this stage. Subsequently, wavy regime occurs, swirling motion is observed at a certain arc length of the bed, while the remaining section forms a static dune. The swirling particle is initiated from one end of the dune and will be accumulated at the back of the dune (refer to Figure 4.3). Further increase in gas velocity results in progressive swirling motion of the bed. This regime is often desired as the interaction between the gas and particle is optimum and the heat and mass transfer rates are at peak. At sufficiently high fluidizing velocity, the particles are entrained gradually, until finally, all particles are blown out from the containing vessel.

During the operation of a relatively deep bed, 2000 g bed loading for instance (Figure 4.2), the packed bed and incipient fluidization regimes are still existed, however, a two-layer bed is observed as claimed by Sreenivasan and Raghavan [13]. These two layers are made up of constantly swirling bottom layer and an aggressively bubbling top layer (Figure 4.4). This is due to the fact that the horizontal force component of the injected gas is attenuated and disappears at the interface between these layers when the gas is flowing through the bed. These layers would, perhaps, be merged to a fully swirling region if the gas velocity is high enough or an entrainment regime might occur when the gas flow rate is increased continuously.

As mentioned earlier in Introduction section, bed pressure drop increases gradually with the increase of air velocity upon minimum fluidization. This distinct feature differentiates the SFB from conventional beds. This relationship indirectly shows that there is an additional downward-acting force besides bed weight that requires to be overcome after incipient fluidization. This extra force is more likely contributed by the increase of the bed wall friction caused by the centrifugal force that pushes the particles towards the bed wall when swirling occurs. The centrifugal force acts horizontally, and normal to the column wall. It has two friction components that are parallel to the wall: One acts to oppose the swirling motion and the other acts downward as centrifugal weight to oppose the upward bed expansion. The pressure drops are predicted to initially decline and will further decease with gas velocity until all particles are blown out from the cylindrical bed.

Besides the bed loadings, the flow pattern is also influenced by the shape and size of the particle. By applying the principle of sand dune formation in desert, the formation of dune is easier (with high angle of repose) to be initiated in the bed particles of high angularity, smaller size, and swallower bed. Particles with greater angularity interlock better with each other, resulting in higher intergranular friction, and meanwhile smaller particles are easier to be carried by the fluidized gas. Therefore, the deep bed (2000 g) of cylindrical particles with the smaller L/D ratio is observed to undergo wavy regime prior to two-layer regime.

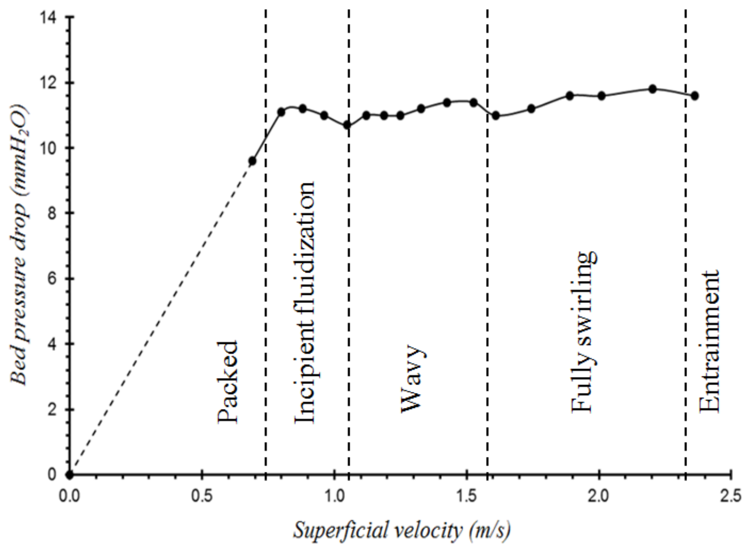

Figure 4.1: Flow regimes for shallow bed (500 g of spherical particle d=2.70 mm at overlap angle of 18°)

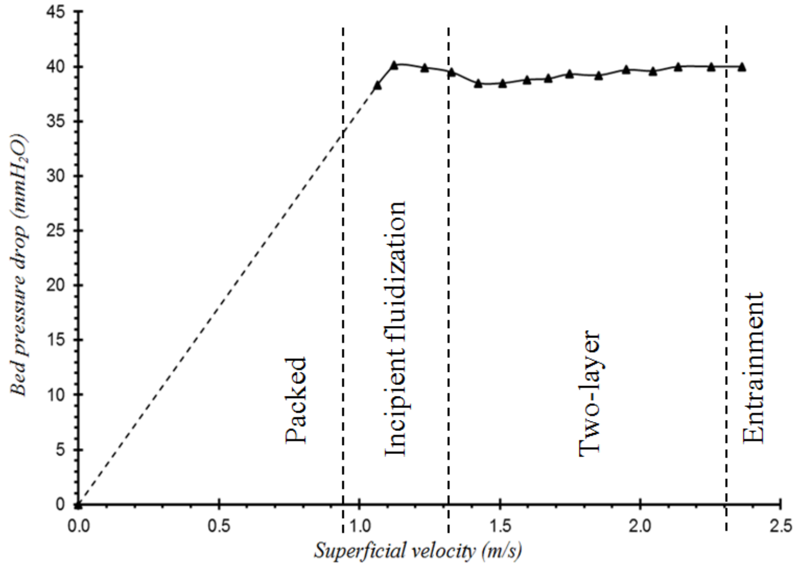

Figure 4.2 : Flow regimes for deep bed (2000 g of irregular shape particle L/D=2.00 at overlap angle of 18°)

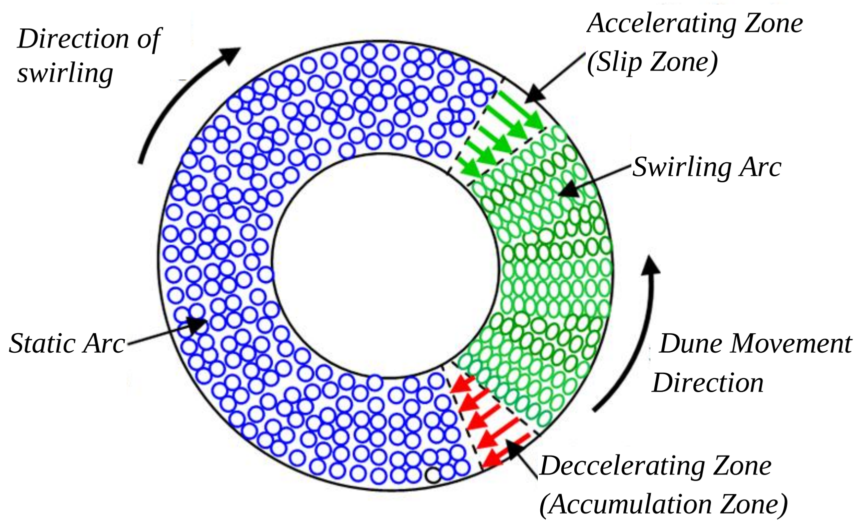

Figure 4.3 : Top view of the bed and distributor

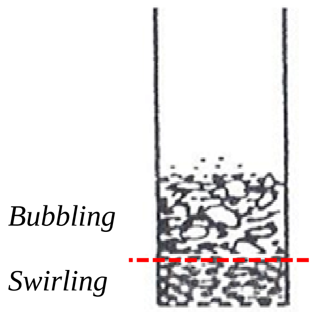

Figure 4.4 : Two-layer regime

4.2 Hysteresis Effect of Bed Pressure Drop

Observing the trend of pressure drop across the bed in the reverse direction (Figure 4.5, 4.6), the particles are defluidized by reducing the air superficial velocity. The operation regime of the particles follows the same patterns as in the forward fluidizing direction corresponding to the value of superficial velocity. During forward fluidization, as the gas velocity increases, the bed pressure drop first shows an upward trend and upon reaching a particular peak value, it drops till it reaches the conventional bed value before starting to rise steadily again because of the frictional resistance due to swirling of the particles. Interestingly, during defluidization, the bed pressure drop decreases without exhibiting a significant hump at incipient fluidization, and its value is lower than the theoretical bed pressure drop indicated by the green dotted line. This can be explained thus: During the forward direction, additional energy is required for perturbing of the 'locked' particles from the packed bed regime in order to get them fluidized. This hysteresis effect suggests that the operation of swirling fluidized bed has history dependent behavior. In fact, if the bed is re-fluidized, the peak in the bed pressure drop would not be seen as the packed bed arrangement had been unlocked permanently during the first fluidization.

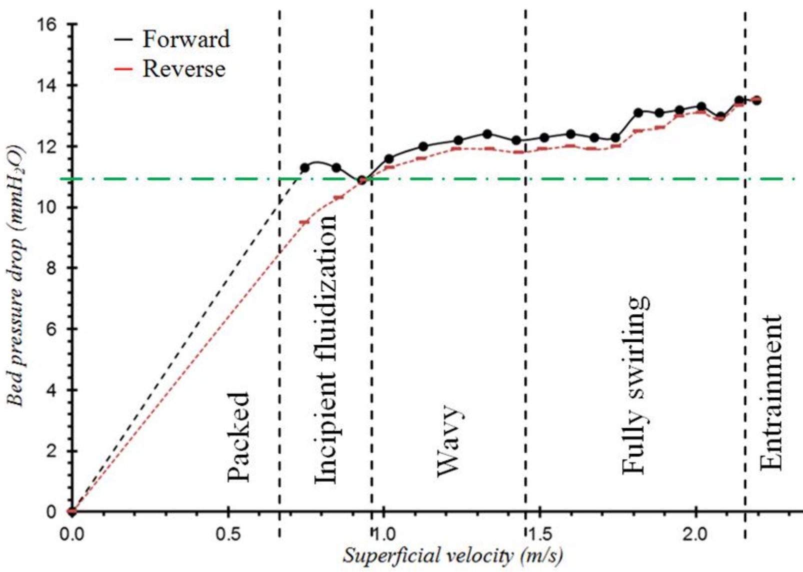

Figure 4.5: Flow regimes for shallow bed (500 g of irregular particle shape with L/D=1.36 mm) at overlap angle of 18°

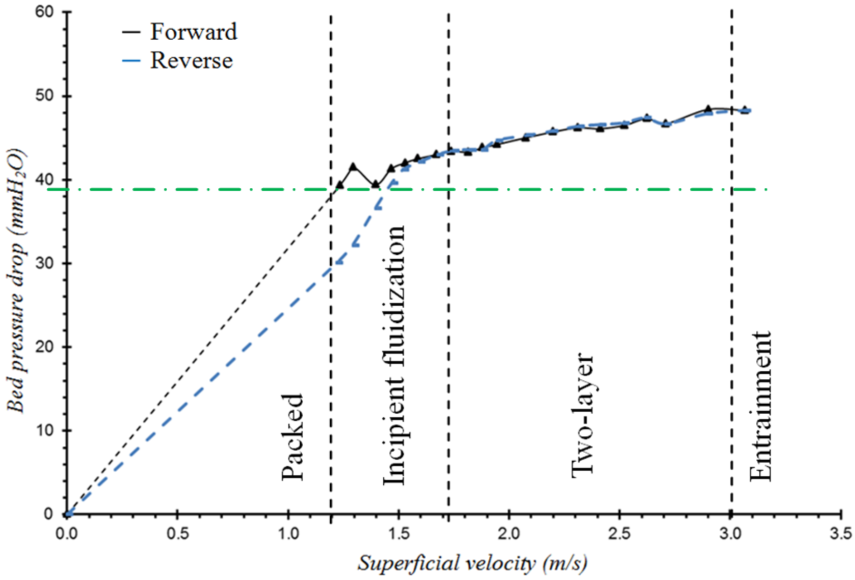

Figure 4.6: Flow regimes for deep bed (2000 g of cylindrical particle with L/D=4.10 mm) at overlap angle of 18°

In calculating the theoretical pressure drop, the author uses correlation recommended by Chitester et al. [25] for coarse particles:

$$\mathrm{Re}_{\mathrm{p,mf}} = \left[(28.7)^2 + 0.0494 Ar\right]^{0.5} - 28.7$$

Where Ar is given by

$$\mathrm{Ar} = \frac{\mathrm{d_p}^3 \rho_{\mathrm{g}} \left(\rho_p - \rho_g\right) g}{\mu_g{}^2}$$

$$U_{mf} = \mathrm{Re}_{p,mf}\, \mu_g \left(\frac{\rho_g}{d_p}\right)$$

Using Ergun Equation [20],

$$\Delta P = \left[\frac{150 \mu_g (1-\varepsilon)^2 U_{mf}}{\varepsilon^3 d_p{}^2} + \frac{1.75(1-\varepsilon)\rho_g U_{mf}{}^2}{\varepsilon^3 d_p}\right] L$$

Where by,

- *ΔP - Pressure drop*
- *Ar - Archimedes number*
- *d_p - Effective diameter of particles*
- *L - Height of bed*
- *ρ_g - Fluidizing gas density*
- *ρ_p - Particle density*
- *g - gravitational acceleration*
- *$Re_{p,\,mf}$ - Reynolds number*
- *ε - Fractional void volume*
- *μ_g - Absolute viscosity of fluidizing gas*
- *U_{mf} - Superficial fluid velocity*

4.3 Effect of Bed Loadings

Bed weights are increased from 500 g to 2000 g in steps of 500 g to study the effect of bed loading (weight) variation, which is also linearly corresponding to the respective bed height. Figures 4.7-4.9 illustrate the trends of bed pressure drop in mm of water against the air superficial velocity with a cone as the center body. The trends clearly indicate that higher bed loading results in higher bed pressure drop for all types of particles shapes and dimensions. The reason of this relationship is that as bed height (or amount of bed particles) increases happens, the amount of particle surface area that requires to be passed by the air before releasing to the bed free surface is also increased. It indirectly shows that in SFB, the bed loading is one of the important parameters to be considered in order to achieve high fluidization quality. In practical situations, the amount of energy provided for fluidization process is often limited, therefore processing a high bed loading may cause poor fluidization quality due to reduced swirling at the upper layer, given specific residence time and energy, and conversely, fluidizing a low bed loading is inefficient in terms of energy utilization.

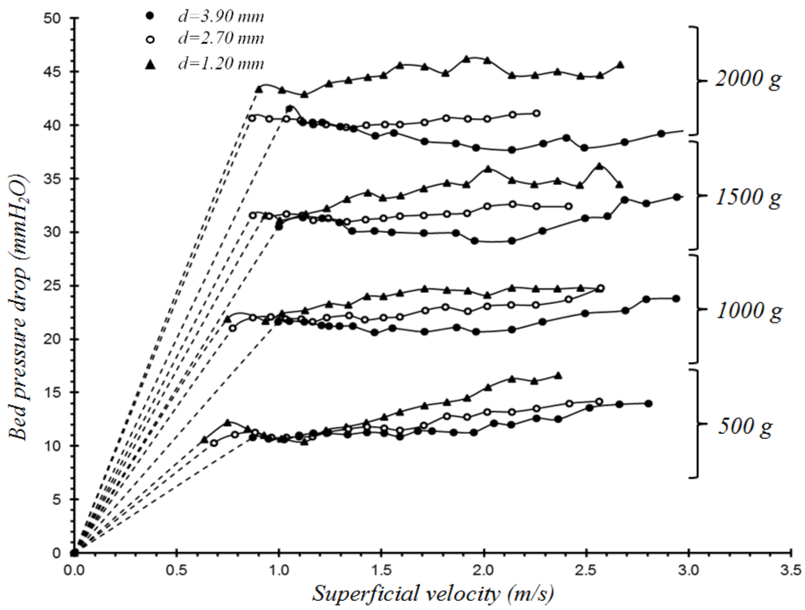

Figure 4.7 : Bed pressure drop against gas superficial velocity for variable bed loading of spherical shape at overlap angle 18°

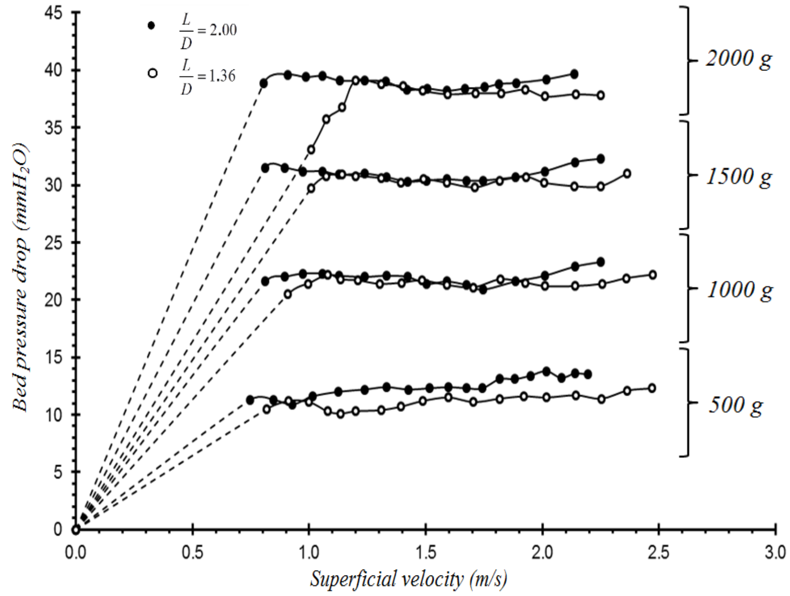

Figure 4.8: Bed pressure drop against gas superficial velocity for variable bed loading of irregular shape at overlap angle 18°

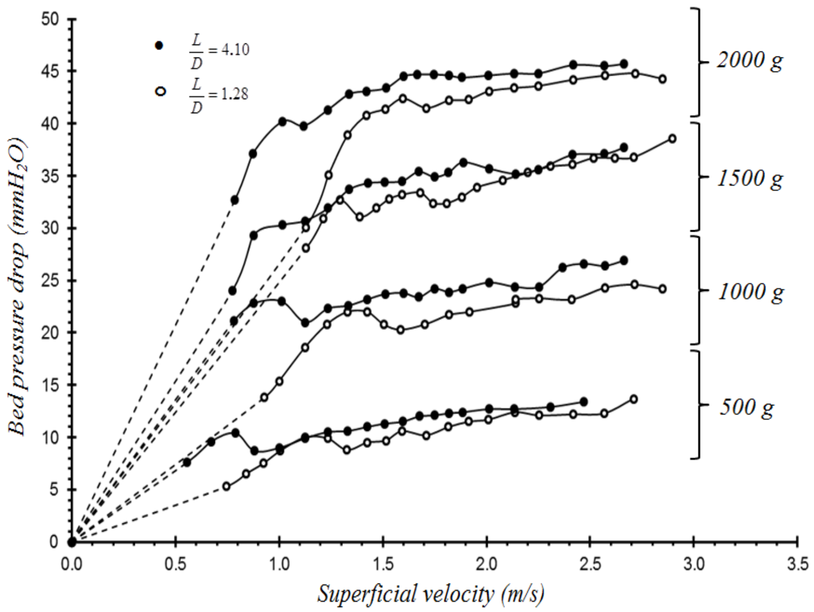

Figure 4.9: Bed pressure drop against gas superficial velocity for variable bed loading of cylindrical shape at overlap angle 18°

4.4 Effect of Particle Size

Figures 4.7-4.9 exemplify the trends of bed pressure drop variation against the air superficial velocity at different particle sizes. The trends clearly show that in the packed region and also fluidization region, larger particles of all shapes have lower pressure drop across the bed. This is due to the fact that smaller size particles in fact have a larger surface area per unit volume. In other words, additional energy is required to overcome the surface friction between particle and fluidizing air when smaller particles are used. The large surface area has greater absorption of angular momentum from the gas to cause more vigorous swirling. Thus, the pressure drop is higher for smaller particles. In addition, larger particles are capable of withstanding higher superficial velocity as the bed expansion occurs slower and thus swirling longer before entrainment occurs [4]. This graph reflects that it is advantageous to use larger particle for fluidization process. On the other hand, a larger interfacial area is good for transport processes. Therefore, rather than dismiss the smaller particles, it will be better to leave the question open: it depends on the particular process, whether it is kinetic-controlled or diffusion-controlled.

4.5 Effect of Particle Shape

A remarkable result is that the cylindrical bed particles require a lower pressure drop relative to other shapes (Figures 4.10-4.13). The plausible reason is that the cylindrical particles tend to rearrange themselves horizontally in a direction transverse to the flow of the fluidizing gas. This result is rather counterintuitive. It would be more normal to believe that the cylindrical particles will assume an orientation in which they will experience less drag, that is, aligned in the flow direction. However, support for the observed behavior comes from the fact that tree logs floating downstream or icebergs at sea take a preferred orientation transverse to the direction of the stream. The constructal theory of natural systems formulated by Professor A. Bejan [26] offers a scientific explanation for the observation.

In engineering terms, the result has practical implications. It shows that in swirling fluidizing beds, with a more deterministic behavior than the conventional fluidized beds with a chaotic behavior, it is advantageous to use solids of cylindrical shape rather than spherical shape, both for the lower bed pressure drop, as well as the higher interfacial area per unit volume for effective transport of heat and species. The spherical shape particles have the highest bed pressure drop followed by irregular shapes. Irregular shape particles have slight "constructal effects" and tend to reposition themselves in a way to facilitate the flow of fluidizing fluid.

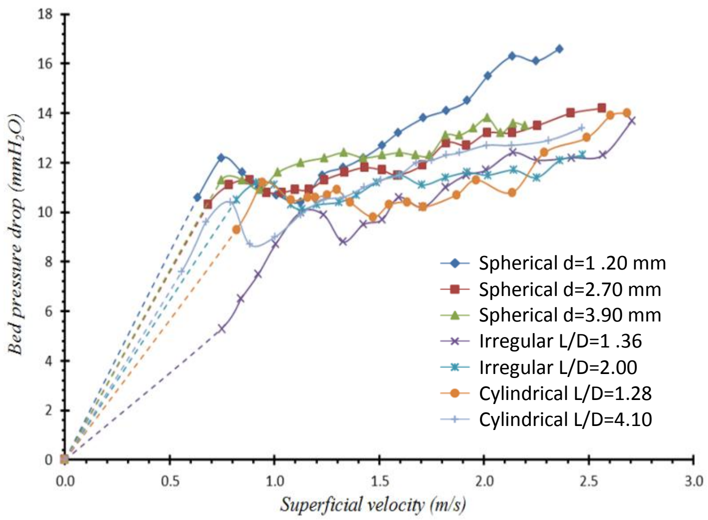

Figure 4.10 : Bed pressure drop against gas superficial velocity for variable particle shape weighted 500 g

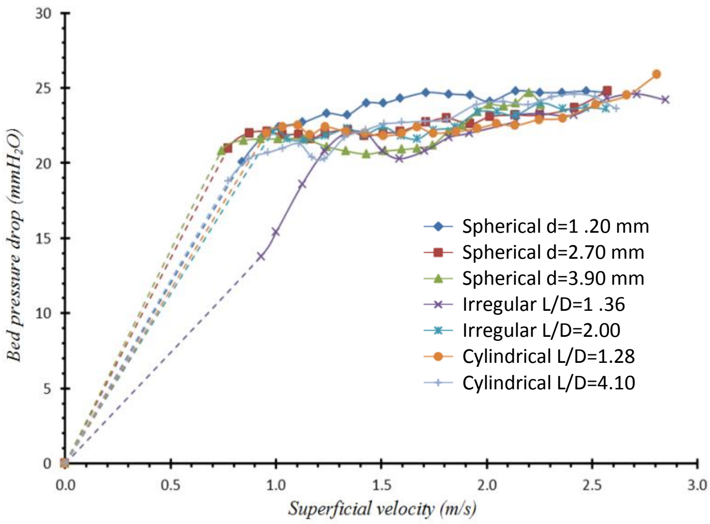

Figure 4.11: Bed pressure drop against gas superficial velocity for variable particle shape weighted 1000 g

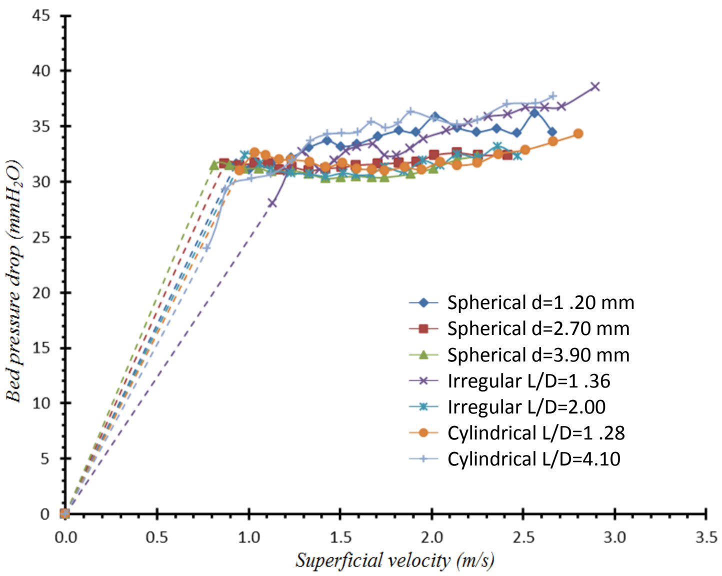

Figure 4.12: Bed pressure drop against gas superficial velocity for variable particle shape weighted 1500 g

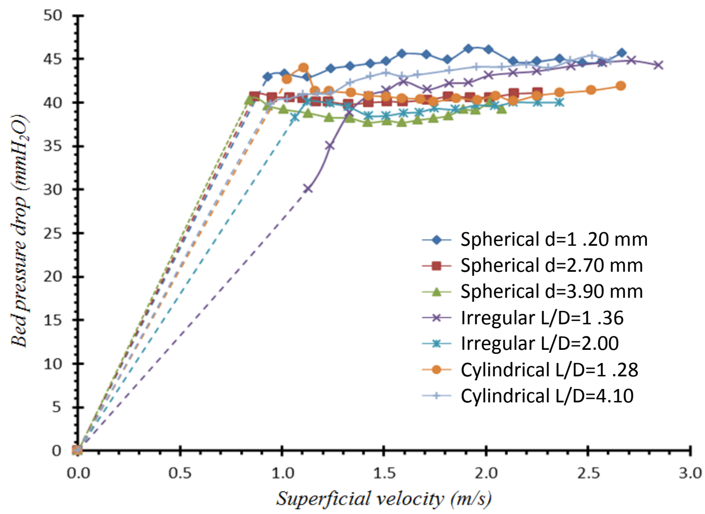

Figure 4.13: Bed pressure drop against gas superficial velocity for variable particle shape weighted 2000 g

4.6 Effect of Blade Overlap Angle

The effect of blade overlap angle variation is insignificant compared to other parameters. Intuitively, the higher overlapping angle is seen to impose higher pressure drop since the air flows through a further blade gap, thus higher friction and resistance.

This parameter does not demonstrate significant relationship in terms of bed pressure drop especially for the spherical and irregular shapes. In fact, these two shapes show a contradictory relationship that higher overlapping angle requires lower pressure drop. The finding yields that this theory is only applicable to the operation of the cylindrical particles. Results are shown in Figures 4.14-4.16.

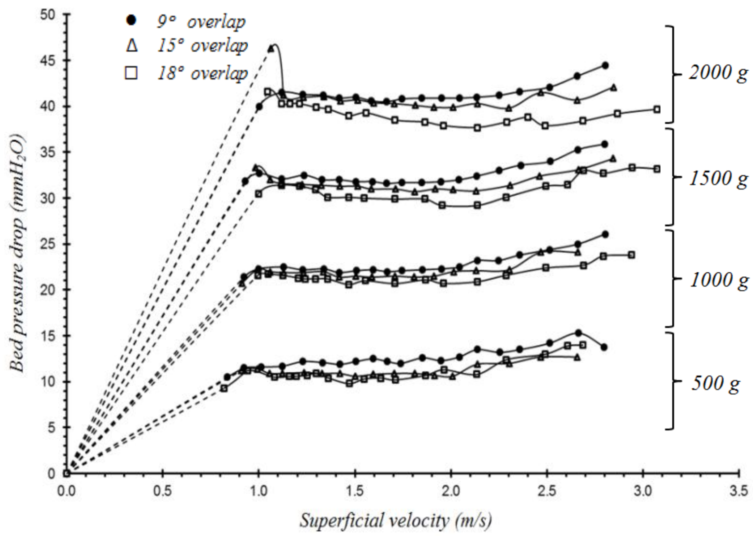

Figure 4.14: Bed pressure drop against gas superficial velocity for variable blade overlap angle with spherical particle d=3.90 mm

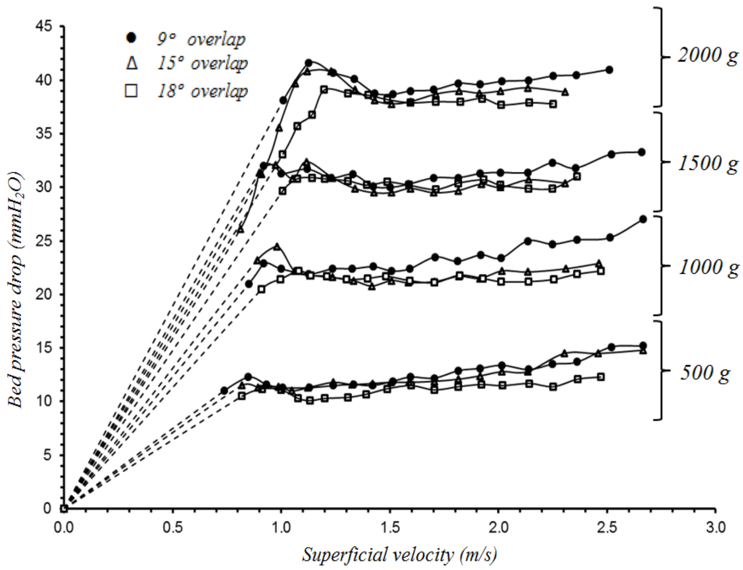

Figure 4.15: Bed pressure drop against gas superficial velocity for variable blade overlap angle with irregular particle shape L/D=2.00

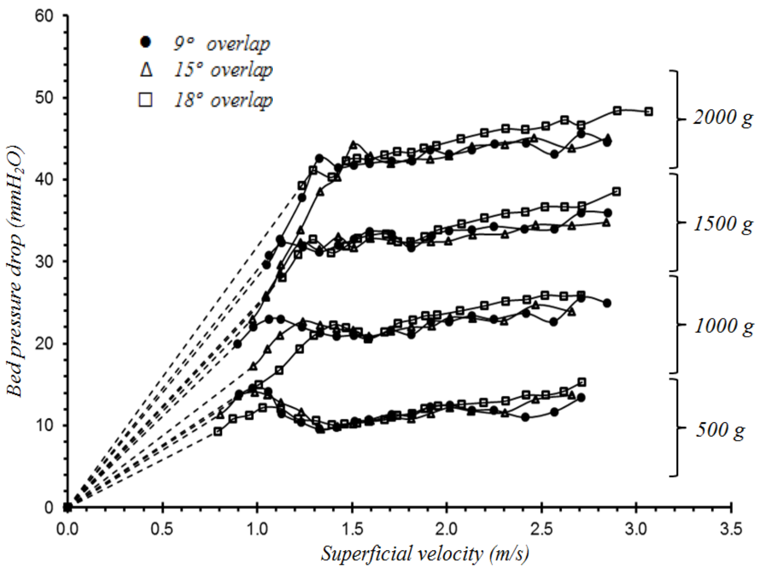

Figure 4.16: Bed pressure drop against gas superficial velocity for variable blade overlap angle with cylindrical particle L/D=4.10

4.7 Distributor Pressure Drop

Logically, as mentioned in the earlier section, the higher overlapping angle may be thought to impose higher pressure drop since the air flows through a longer blade gap, with higher friction and resistance [16]. However, from the experimental results as illustrated in Figure 4.17, it seems that the friction is not the dominant parameter in determinining this pressure drop, the flow pattern of the gas injected from the blade gap is the main factor in this case. The further blade gap is able to drive the injection of gas into the desired inclination more effectively after dispersing from the distributor (Figure 4.18). The blade inclination angle is θ but the gas exits from the blades at a larger angle α. This is due to the growth of the boundary layer that is not symmetrical on the two blades. With longer overlap angle. i.e., longer blades, the flow tends more to fully developed flow. It is anticipated that this effectiveness peaks at a certain overlap angle and a higher pressure drop will occur due to the friction. The same concept applies to inclination angle, in which upwards flow from plenum chamber experiences more change in direction when entering the distributor at lower inclination. Thus, distributor pressure drop is significantly lower at higher inclination angle.

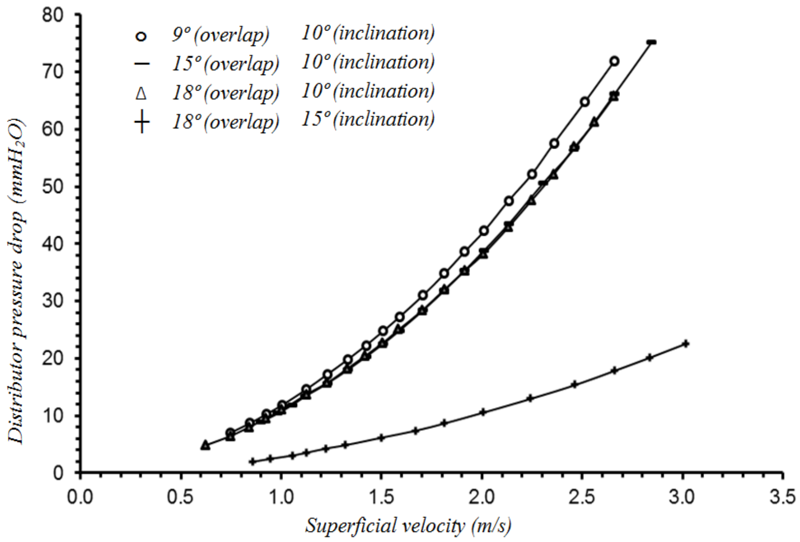

Figure 4.17: Distributor pressure drop for variable blade overlap and inclination angles, fluidizing gas direction after dispersing through empty bed

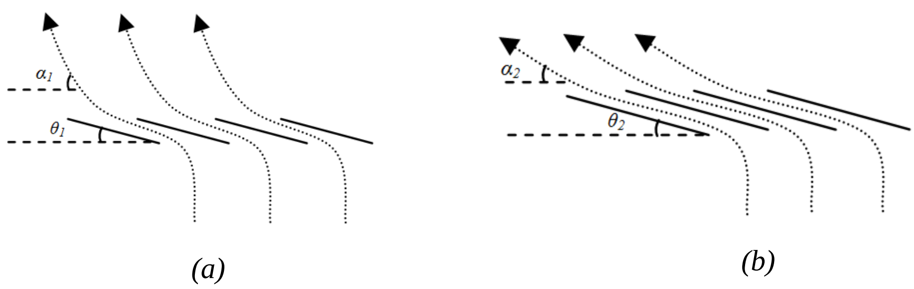

Figure 4.18 (a)-(b): Injection of gas at (a) smaller blade overlap angle, (b) larger blade overlap angle

4.8 Slugging Period

In the wavy regime, at a certain superficial velocity, the particles begin to pile up causing a dune to form. Air continues to move particles up to the pile until the pile is so steep that it collapses under its own weight. The collapsing particles come to rest when it reaches just the right steepness to keep the dune stable. The particles at the slip region will be carried by the fluidizing gas in circular path and accumulate at the other side of dune. This causes the coriolis effect that the dune moves in the opposite direction with the fluidizing gas. Referring to the trend of the slugging time in Figure 4.20, this parameter is mainly affected by the variation of bed loadings and particles sizes. In relatively small and shallow loading, the formation of the dune occurs at lower air velocity and they tend to accumulate with each other rather than slip away, causing another side of arc unfilled as the volume of bed is small. Thus, the overall dune movement is slow. During the increasing of gas velocity, the height of the dune becomes lower as more particles from the slip face are brought to the other side via the empty arc, causing the dune to elongate. This elongation brings the effect that the movement of the dune becomes faster as it moves and at the same time it extends, until the dune is low enough to be brought to swirl and this marks the occurrence of next regime (Figure 4.19(a) and Figure 4.3).

In a bed of large particles and high loading, the increasing of gas superficial velocity also encourages the slip face to slip, then swirl and accumulate at the other end. However, the remaining arc is filled by particle with lower level, the height of the dune decreases with the increasing of air velocity, and the remaining arc increases in height, until it reaches the next regime where both are at the same level. The slugging time becomes longer with the increasing of gas velocity due to the absence of the elongation occurrence and when the particles height of the remaining arc becomes higher, it is more difficult for the fluidizing gas to carry the particle to form dune (Figure 4.19(b)).

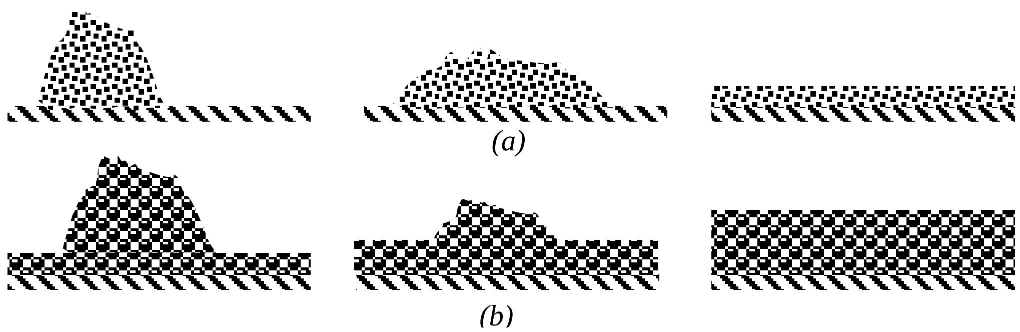

Figure 4.19 (a)-(b): Slugging regimes in circumferential view for bed of (a) small particle and shallow loading and (b) large particle and deep loading

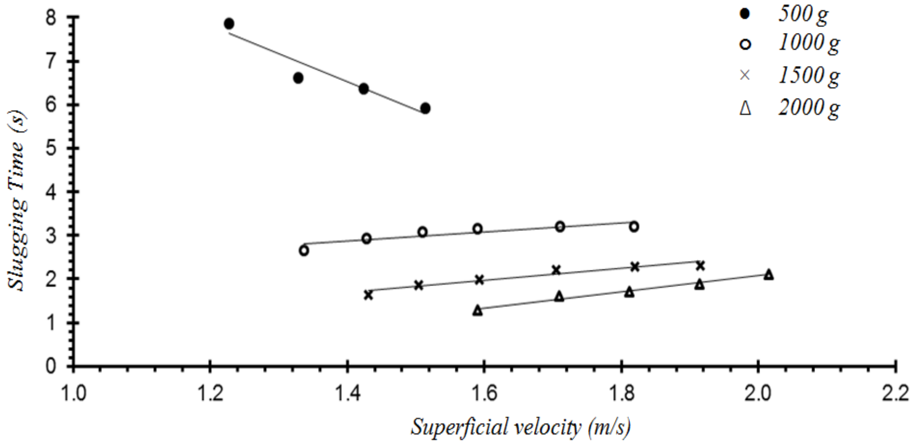

(a)

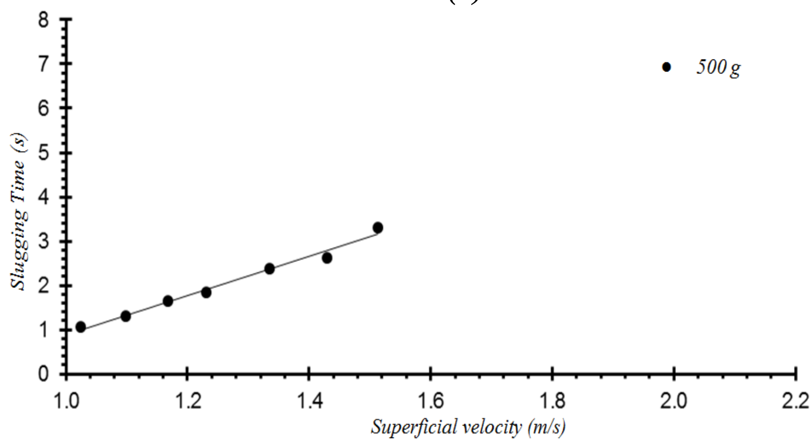

(b)

Figure 4.20(a)-(b): Slugging time for (a) sphere particle d=1.2 mm, (b) sphere particle d=3.9 mm, at overlap angle of 18°

4.9 Effect of Blade Inclination Angle

In the case of blade inclination angle, the value of pressure drop represents the flow resistance of the bed and the momentum transferred from gas to the particles (and to the kinetic energy gained by the particles as a result).

When the air enters at smaller inclination, it has a greater angular momentum and causes a more vigorous swirling of the bed particles. This can be observed visually. So, with more momentum transferred from the air, its pressure drop is higher. Therefore, from the bed pressure drop trend in Figure 4.21, larger inclination angle has lower bed pressure drop due to the lower momentum transferred to the particles.

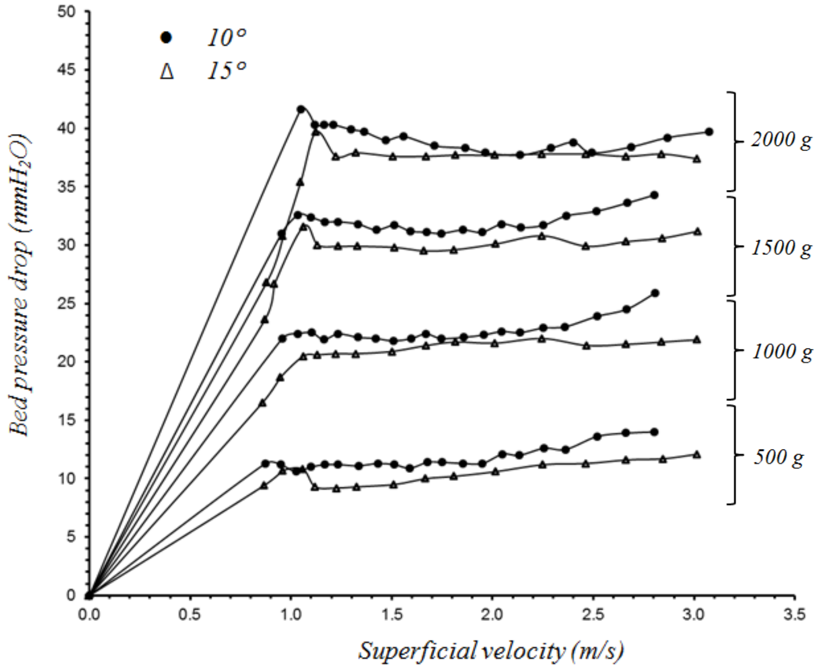

Figure 4.21 : Bed pressure drop against gas superficial velocity for variable blade inclination angle with spherical particle d=3.90 mm

CHAPTER 5

CONCLUSIONS AND RECOMMENDATIONS

In the thorough analysis of raw data, the hydrodynamics behavior of the novel gas-particle contacting technique of the SFB has been studied through a series of experiments. The findings indicate that:

i. The order of flow regimes in SFB with shallow bed are packed bed, incipient fluidization, wavy regime, and finally entrainment regime. Meanwhile the deep bed is prone to undergo a two-layer regime before the particles are entrained.
ii. The bed pressure drop exhibits hysteresis effect at incipient conditions which indicates that the operation of swirling fluidized bed is history dependent.
iii. Higher bed loading has higher bed pressure drop, hence requires more energy for fluidization.
iv. Larger solid particles size have lower pressure drop of bed and capable of withstanding the condition of high gas superficial velocity.
v. Cylindrical particles have the lowest bed pressure drop among all the shapes as they have the tendency to position themselves to facilitate the flowing fluid.
vi. Larger blade overlapping angle imposes additional pressure drop, particularly at the distributor since the air is now forced to flow through higher resistance.
vii. Particle size, shape, and bed weight are the most significant variables that have more impact on the bed characteristics, while the blade dimension has relatively smaller effect on the bed behavior.
viii. The slugging time is affected by the effect of the bed loading, particle size and particle shape.
ix. Larger overlap angle and larger blade inclination angle exhibit lower distributor pressure drop.
x. Smaller inclination angle of gas injection has higher bed pressure drop.

To conclude, this project is a comprehensive experimental study of hydrodynamic characteristics of swirling fluidized beds. Based on boiled down deadlines, and target dates as listed in the Gantt chart, the overall research progress is notable and reaching the target. Research set up is installed as design and the primary data which is analyzed and interpreted shows interesting results and considerably accurate to show the influence of each parameter on the bed behavior. In short, this project is definitely feasible to be completed within the study timeframe with its undeniable significance towards fluidization engineering. The parameter of blades configurations in terms of inclination angle will be studied in details later as the blades and the support rings require complex fabrication process. The author recommends that the hydrodynamics of newly invented multistage bed to be studied in comparison with to the single stage bed, as this study may perhaps contribute in revealing the rationale on of the energy conservation technology. Perhaps, in future study, particle tracking velocimetry (PTV) can be used to investigate the interstitial motion of individual particles and its relations with the characteristic flow structures formed in fluidized beds without disturbing the flow field.

CHAPTER 6

BIBLIOGRAPHY

[1] W.C. Yang, *Handbook of Fluidization and Fluid-Particle,* USA: Systems CRC Press, 2003, pp. 67−69.

[2] V. R. Raghavan, M. Kind and H. Martin, "Modeling of the Hydrodynamics of Swirling Fluidized Beds", in *4th European Thermal Sciences Conf,* 'EUROTHERM' and Heat Exchange Engineering Exhibition, Birmingham, UK, 29-31 March 2004.

[3] K. V. Vinod, M. Jeevaneswary, and V. R. Raghavan, "Experimental Studies on the Effect of Blade Overlap Angle on Bed Pressure Drop in a Swirling Fluidized Bed" in *Int. Conf. on Plant, Equipment and Reliability,* Kuala Lumpur, Malaysia, 2010.

[4] D. Kunii and O. Levenspiel, *Fluidization Engineering,* 2nd Ed., London: Butter Worth-Heinemann, 1991, pp: xix.

[5] J. C. Schouten, and C. M. Van den Bleek, "Monitoring the Quality of Fluidization Using the Short-Term Predictability of Pressure Fluctuations", AIChE Journal, Jan. 1998, vol. 44, 48, no. 1.

[6] M. Jeevaneswary, "Experimental Studies on the Effect of the Particle Shape and Distributor Blade Overlap Angle on the Bed Pressure Drop in a Swirling Fluidized Bed," BEng. dissertation, Dept. Mech. Eng., Universiti Teknologi PETRONAS, Perak, Malaysia, May 2011.

[7] K. V. Vinod and V. R. Raghavan, "Developments in fluidized bed technology – A Review", *Proc. IEEE,* 2011.

[8] R. L. Pigford and T. Baron, "Hydrodynamic Stability of a Fluidized Bed", I&EC Fundamentals, Feb. 1965, pp. 81-87, vol. 4, no. 1.

[9] M. Faizal, K. V. Vinod and V.R. Raghavan, “Experimental Studies on a Swirling Fluidized Bed with Annular Distributor”, in *Int. Conference on Plant, Equipment and Reliability,* Kuala Lumpur, Malaysia, June 15-17 2010.

[10] D. P. Stocker, J. E. Brooker, E. N. Zingarelli and U. Hedge, “Effects of Gravity on Swirl-Stabilized Fluidized Beds” in *44th American Ins. of Aeronautics and Astronautics Aerospace Sciences Meeting and Exhibition*, Reno, Nevada, Jan 2006.

[11] L.T. Fan, C.C. Chang, and Y.S. Yu, “Incipient Fluidization Condition for a Centrifugal Fluidized Bed”, AIChE. Journal, June 1985, pp. 999, vol. 31, no. 6.

[12] J. R. Howard, *Fluidized Bed Technology: Principles and Applications,* New York, NY: Adam Higler, 1989.

[13] B. Sreenivasan and V.R. Raghavan, “Hydrodynamics of a Swirling Fluidized Bed”, Chemical Engineering and Processing, 2002, pp. 41, 99-106.

[14] F. Ouyang and O. Levenspiel, “Spiral Distributor for Fluidized Beds”, Ind. Eng. Chem. Process Design Develop., 1986, pp. 1986, vol 25.

[15] M. M. Paulose, “Hydrodynamic Study of Swirling Fluidized Bed and The Role of Distributor”, School of Eng., Cochin University of Sci. and Technology, Kerala, India, 2006.

[16] J. Shu, V.I. Lakshmanan and C.E. Dodson, “Hydrodynamic study of a toroidal fluidized bed reactor, Chemical Engineering and Processing”, 2000, pp. 39, 499-506.

[17] M.F.M. Batcha and V.R. Raghavan, “Experimental Studies on a Swirling Fluidized Bed with Annular Distributor”, Journal of Applied Sciences, 2011, 11: 1980-1986.

[18] R. Kaewklum and V. I. Kuprianov, “Experimental studies on a novel swirling fluidized bed combustor using an annular spiral distributor”, pp. 89: 43-52, 2010.

[19] C. Sobrino, J.A. Almendros-Ibañez, D. Santana and M. de Vega, “Fluidization of Group B particles with a rotating distributor”, Powder Technology, 2007, pp. 181, 273–280.

[20] S. Ergun, “Fluid Flow through Packed Columns”, Carnegie Institute of Technology, Pittsburgh, Pennsylvania, 1986.

[21] J. W. Hiby, “Periodic Phenomena Connected with Gas-Solid Fluidization”, in *Int. Proc. Int. Symp. on Fluidization*, Eindhoven, 1967, pp. 99.

[22] D. Geldart and J. Baeyens, “The Design of Distributors for Gas-Fluidized Beds”, Powder Technology, 1985, pp. 67−78.

[23] K.V. Vinod and V. R. Raghavan, “Operation of a Swirling Fluidized Bed – the Effect of Wall-bed Heat Transfer, Particle Shape, Size and Blade Overlap”, in *21st National & 10th ISHMT-ASME Heat and Mass Transfer Conference*, IIT Madras, India, December 27−30, 2011.

[24] Y. Peng, L. T. Fan, “Hydrodynamic characteristics of fluidization in liquid–solid tapered beds” Chemical Engineering Science, pp. 2277 – 2290, vol. 52, no. 14, 1997.

[25] D.C. Chitester, R.M. Kornosky, L.S. Fan, “Characteristics of fluidisation at high pressure” Chemical Engineering Science 39, pp. 253, 1984.

[26] Bejan, A, “Shape and Structure, from Engineering to Nature”, Cambridge University Press, Cambridge, UK, 2000.

CHAPTER 7

APPENDICES

APPENDIX A: EXAMPLE OF SUPERFICIAL VELOCITY CALCULATION

Example of superficial velocity calculation for spherical particle, d=2.7 mm at 500g

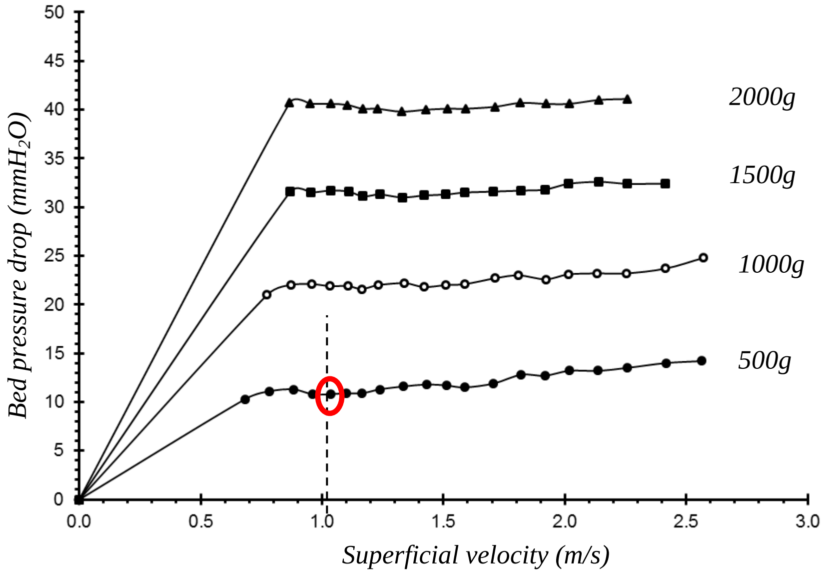

Figure 7.1: Bed pressure drop against superficial velocity for variable bed loading for spherical particle, d=2.7 mm

At the circled point,

Pressure drop across orifice plate is 20.1 mmH_2O (reading taken from differential pressure transmitter),

From the orifice calculation,

$$
\begin{aligned}
\text{Superficial Velocity, } V_{\text{superficial}} &= 0.2249\sqrt{\text{Pressure difference, } \Delta P} \\
&= 0.2249\sqrt{20.1} \\
&= 1.01\ m/s \text{ (as shown is Figure 7.1)}
\end{aligned}
$$

APPENDIX B: PARTIAL EXPERIMENT RAW DATA *(Table 7.3)*

Shape: Spherical Size: d=1.2mm Mass: 500g Inclination: 10deg Overlap: 18deg

Data No.	ΔP across orifice		Superfical Velocity		ΔP across distributor	ΔP across distributor with particle		ΔP across bed		Slugging Time					Observation
	Forward	Reverse	Forward	Reverse		Forward	Reverse	Forward	Reverse	T1	T2	T3	T4	Tavg	
	mmH_2O	mmH_2O	m/sec	m/sec	mmH_2O	mmH_2O	mmH_2O	mmH_2O	mmH_2O	s	s	s	s	s	
1	7.900	8.300	0.693	0.711	4.500	15.100	11.200	10.600	6.700						Incipient
2	11.000	10.700	0.818	0.807	6.100	18.300	15.600	12.200	9.500						Bubbling
3	14.100	14.300	0.926	0.933	7.700	19.300	17.600	11.600	9.900						Bubbling
4	16.900	17.400	1.014	1.029	9.200	20.200	21.400	11.000	12.200						Bubbling
5	20.100	20.400	1.106	1.114	10.700	21.400	21.500	10.700	10.800						Bubbling
6	24.900	25.300	1.231	1.241	13.400	23.800	23.800	10.400	10.400						Bubbling
7	29.700	30.100	1.345	1.354	15.400	26.900	26.600	11.500	11.200	7.830	7.990	7.670	7.930	7.855	Slugging
8	34.800	35.000	1.455	1.460	17.900	29.700	29.400	11.800	11.500	6.600	6.550	6.620	6.740	6.628	Slugging
9	40.000	40.500	1.560	1.570	20.100	32.300	32.400	12.200	12.300	6.330	6.470	6.350	6.330	6.370	Slugging
10	45.200	45.300	1.659	1.661	22.400	35.100	35.200	12.700	12.800	5.760	6.050	5.970	5.850	5.908	Slugging
11	49.800	50.000	1.741	1.745	24.700	37.900	37.900	13.200	13.200						Swirling
12	57.700	57.500	1.874	1.871	28.100	41.900	41.700	13.800	13.600						Swirling
13	65.200	65.500	1.992	1.997	31.700	45.800	46.000	14.100	14.300						Swirling
14	72.600	72.300	2.102	2.098	35.100	49.600	49.500	14.500	14.400						Swirling
15	80.300	80.400	2.211	2.212	38.000	53.500	53.300	15.500	15.300						Swirling
16	90.000	90.000	2.341	2.341	42.600	58.900	58.800	16.300	16.200						Entrrain
17	99.600	100.000	2.462	2.467	47.300	63.400	63.400	16.100	16.100						Entrrain
18	109.900	-	2.586	-	51.800	68.400	-	16.600	-						Entrrain

Shape: Spherical Size: d=1.2mm Mass: 1000g Inclination: 10deg Overlap: 18deg

Data No.	ΔP across orifice		Superfical Velocity		ΔP across distributor	ΔP across distributor with particle		ΔP across bed		Slugging Time					Observation
	Forward	Reverse	Forward	Reverse		Forward	Reverse	Forward	Reverse	T1	T2	T3	T4	Tavg	
	mmH_2O	mmH_2O	m/sec	m/sec	mmH_2O	mmH_2O	mmH_2O	mmH_2O	mmH_2O	s	s	s	s	s	
1	13.900	13.600	0.920	0.910	8.100	28.200	27.200	20.100	19.100						Incipient
2	17.200	17.000	1.023	1.017	9.600	31.300	31.000	21.700	21.400						Start bubbling
3	20.200	19.800	1.109	1.098	11.100	33.500	33.200	22.400	22.100						Bubbling
4	25.000	24.900	1.234	1.231	13.800	36.500	35.900	22.700	22.100						Bubbling
5	30.400	30.000	1.360	1.351	15.800	39.100	38.300	23.300	22.500						Bubbling
6	35.200	35.400	1.464	1.468	18.300	41.500	41.600	23.200	23.300	2.720	2.680	2.600	2.680	2.670	Slugging
7	40.200	40.500	1.564	1.570	20.500	44.500	44.500	24.000	24.000	2.890	2.980	2.970	2.890	2.933	Slugging
8	44.900	45.400	1.653	1.662	22.800	46.800	46.700	24.000	23.900	3.050	3.010	3.110	3.140	3.078	Slugging
9	49.800	49.600	1.741	1.738	25.100	49.400	48.700	24.300	23.600	3.160	3.170	3.230	3.090	3.163	Slugging
10	57.700	57.300	1.874	1.868	28.500	53.200	52.400	24.700	23.900	2.980	2.960	3.050	3.080	3.018	Slugging
11	65.200	64.600	1.992	1.983	32.100	56.700	56.700	24.600	24.600	3.030	3.010	3.010	3.050	3.025	Slugging
12	72.800	72.500	2.105	2.101	35.400	59.900	60.500	24.500	25.100						Swirling
13	80.000	80.000	2.207	2.207	38.400	62.500	63.500	24.100	25.100						Swirling
14	89.900	90.300	2.339	2.345	43.000	67.800	67.800	24.800	24.800						Swirling
15	100.000	100.000	2.467	2.467	47.700	72.400	72.700	24.700	25.000						Swirling
16	109.600	110.000	2.583	2.588	52.200	76.900	76.700	24.700	24.500						Swirling
17	120.400	120.200	2.707	2.705	57.000	81.800	81.500	24.800	24.500						Entrrain
18	129.600	-	2.809	-	61.300	86.000	-	24.700	-						Entrrain

Shape: Spherical Size: d=1.2mm Mass: 1500g Inclination: 10deg Overlap: 18deg

Data No.	ΔP across orifice		Superfical Velocity		ΔP across distributor	ΔP across distributor with particle		ΔP across bed		Slugging Time				Observation
	Forward	Reverse	Forward	Reverse		Forward	Reverse	Forward	Reverse	T1	T2	T3	Tavg	
	mmH_2O	***mmH_2O***	***m/sec***	***m/sec***	***mmH_2O***	***mmH_2O***	***mmH_2O***	***mmH_2O***	***mmH_2O***	***s***	***s***	***s***	***s***	
1	17.100	16.800	1.020	1.011	9.600	41.200	39.700	31.600	30.100					Incipient
2	19.800	19.800	1.098	1.098	11.100	42.200	41.400	31.100	30.300					Bubbling
3	25.100	24.900	1.236	1.231	13.800	45.500	45.400	31.700	31.600					Bubbling
4	30.000	30.500	1.351	1.363	15.800	48.000	48.000	32.200	32.200					Bubbling
5	34.900	34.900	1.458	1.458	18.300	51.400	51.000	33.100	32.700					Bubbling
6	40.400	40.400	1.568	1.568	20.500	54.200	54.200	33.700	33.700	1.730	1.600	1.600	1.640	Slugging
7	44.600	44.600	1.648	1.648	22.800	56.000	55.900	33.200	33.100	1.850	1.780	1.740	1.860	Slugging
8	50.000	49.800	1.745	1.741	25.100	58.500	58.600	33.400	33.500	1.970	2.040	2.100	1.980	Slugging
9	57.300	57.600	1.868	1.873	28.500	62.600	62.700	34.100	34.200	2.280	2.230	2.240	2.220	Slugging
10	65.300	65.400	1.994	1.995	32.100	66.700	66.300	34.600	34.200	2.400	2.300	2.350	2.220	Slugging
11	72.300	72.200	2.098	2.096	35.400	69.900	69.600	34.500	34.200	2.460	2.450	2.480	2.320	Slugging
12	80.400	79.900	2.212	2.205	38.400	74.300	73.300	35.900	34.900	Minor slugging				Slugging
13	90.100	89.900	2.342	2.339	43.000	77.900	77.500	34.900	34.500					Swirling
14	99.600	99.800	2.462	2.465	47.700	82.200	82.400	34.500	34.700					Swirling
15	109.600	109.700	2.583	2.584	52.200	87.000	87.000	34.800	34.800					Swirling
16	120.000	119.700	2.703	2.699	57.000	91.400	91.100	34.400	34.100					Swirling
17	129.700	129.800	2.810	2.811	61.300	97.500	97.400	36.200	36.100					Entrrain
18	139.700	-	2.916	-	65.900	100.400	-	34.500	-					Entrrain

Shape: Spherical Size: d=1.2mm Mass: 2000g Inclination: 10deg Overlap: 18deg

Data No.	ΔP across orifice		Superfical Velocity		ΔP across distributor	ΔP across distributor with particle		ΔP across bed		Slugging Time				Observation
	Forward	Reverse	Forward	Reverse		Forward	Reverse	Forward	Reverse	T1	T2	T3	Tavg	
	mmH_2O	***mmH_2O***	***m/sec***	***m/sec***	***mmH_2O***	***mmH_2O***	***mmH_2O***	***mmH_2O***	***mmH_2O***	***s***	***s***	***s***	***s***	
1	17.000	17.100	1.017	1.020	9.600	52.500	48.700	42.900	39.100					Incipient
2	20.200	19.600	1.109	1.092	11.100	54.400	52.600	43.300	41.500					Bubbling
3	24.900	25.100	1.231	1.236	13.800	56.700	56.300	42.900	42.500					Bubbling
4	30.400	30.300	1.360	1.358	15.800	59.700	59.100	43.900	43.300					Bubbling
5	35.200	35.300	1.464	1.466	18.300	62.500	61.900	44.200	43.600					Bubbling
6	40.400	40.200	1.568	1.564	20.500	65.000	64.800	44.500	44.300					Swirling
7	44.900	44.900	1.653	1.653	22.800	67.500	67.300	44.700	44.500					Swirling
8	49.800	50.200	1.741	1.748	25.100	70.700	70.300	45.600	45.200	1.250	1.350	1.300	1.280	Entrrain
9	57.600	57.700	1.873	1.874	28.500	74.000	74.400	45.500	45.900	1.650	1.580	1.580	1.610	Entrrain
10	64.700	64.800	1.985	1.986	32.100	77.000	77.000	44.900	44.900	1.660	1.710	1.700	1.720	Entrrain
11	72.200	72.500	2.096	2.101	35.400	81.600	81.800	46.200	46.400	1.860	1.910	1.910	1.900	
12	80.000	80.000	2.207	2.207	38.400	84.500	84.600	46.100	46.200	2.140	2.170	2.100	2.210	
13	89.900	89.600	2.339	2.335	43.000	87.700	88.400	44.700	45.400	Minor slugging				
14	99.800	100.500	2.465	2.473	47.700	92.400	92.900	44.700	45.200					
15	109.800	110.500	2.585	2.594	52.200	97.200	97.800	45.000	45.600					Entrrain
16	120.500	120.500	2.708	2.708	57.000	101.600	101.500	44.600	44.500					Entrrain
17	129.900	130.200	2.812	2.815	61.300	105.960	106.800	44.660	45.500					Entrrain
18	140.100	-	2.920	-	65.900	111.600	-	45.700	-					Entrrain

Shape: Spherical Size: d=2.7mm Mass: 500g Inclination: 10deg Overlap: 18deg

Data No.	ΔP across orifice		Superfical Velocity		ΔP across distributor	ΔP across distributor with particle		ΔP across bed		Slugging Time					Observation
	Forward	Reverse	Forward	Reverse		Forward	Reverse	Forward	Reverse	T1	T2	T3	T4	Tavg	
	mmH_2O	*mmH_2O*	*m/sec*	*m/sec*	*mmH_2O*	*mmH_2O*	*mmH_2O*	*mmH_2O*	*mmH_2O*	*s*	*s*	*s*	*s*	*s*	
1	9.400	9.600	0.756	0.764	5.600	15.200	15.500	9.600	9.900						Incipient
2	12.600	12.600	0.876	0.876	7.000	18.100	18.200	11.100	11.200						Bubbling
3	15.300	15.300	0.965	0.965	8.500	19.700	19.800	11.200	11.300						Bubbling
4	18.200	18.400	1.053	1.058	10.100	21.100	21.300	11.000	11.200						Start swirling
5	21.700	22.000	1.149	1.157	11.600	22.300	22.700	10.700	11.100	1.750	1.880	1.850	1.820	1.825	Slugging
6	24.700	24.400	1.226	1.219	12.800	23.800	23.900	11.000	11.100	2.120	2.150	2.150	2.120	2.135	Slugging
7	27.800	27.600	1.301	1.296	14.300	25.300	25.500	11.000	11.200	2.410	2.310	2.310	2.280	2.328	Slugging
8	30.700	31.100	1.367	1.376	15.900	26.900	27.000	11.000	11.100	2.660	2.600	2.630	2.500	2.598	Slugging
9	34.700	34.800	1.453	1.455	17.700	28.900	28.900	11.200	11.200	3.600	3.440	3.280	3.410	3.433	Slugging
10	40.000	40.300	1.560	1.566	20.000	31.400	31.700	11.400	11.700						Swirling
11	45.900	46.300	1.672	1.679	22.800	34.200	34.400	11.400	11.600						Swirling
12	51.100	51.500	1.764	1.771	25.700	36.700	36.800	11.000	11.100						Swirling
13	60.000	59.900	1.911	1.910	29.500	40.700	41.100	11.200	11.600						Swirling
14	70.300	70.600	2.069	2.073	33.900	45.500	45.900	11.600	12.000						Swirling
15	79.600	80.100	2.201	2.208	38.600	50.200	50.100	11.600	11.500						Swirling
16	95.700	95.600	2.414	2.412	45.700	57.500	57.400	11.800	11.700						Swirling
17	109.900	-	2.586	-	52.300	63.900	-	11.600	-						Entrain

Shape: Spherical Size: d=2.7mm Mass: 1000g Inclination: 10deg Overlap: 18deg

Data No.	ΔP across orifice		Superfical Velocity		ΔP across distributor	ΔP across distributor with particle		ΔP across bed		Slugging Time				Observation
	Forward	Reverse	Forward	Reverse		Forward	Reverse	Forward	Reverse	T1	T2	T3	Tavg	
	mmH_2O	*mmH_2O*	*m/sec*	*m/sec*	*mmH_2O*	*mmH_2O*	*mmH_2O*	*mmH_2O*	*mmH_2O*	*s*	*s*	*s*	*s*	
1	11.100	11.100	0.822	0.822	6.300	26.300	26.500	20.000	20.200					Incipient
2	15.300	15.500	0.965	0.971	8.500	30.600	30.800	22.100	22.300					Bubbling
3	19.000	19.200	1.075	1.081	10.100	32.500	32.700	22.400	22.600					Bubbling
4	21.400	21.700	1.141	1.149	11.600	33.600	33.800	22.000	22.200					Bubbling
5	27.500	28.200	1.294	1.310	14.300	36.300	36.600	22.000	22.300					Bubbling
6	34.600	35.100	1.451	1.462	17.700	39.500	40.300	21.800	22.600					Start swirling
7	39.700	39.800	1.555	1.557	20.000	41.800	41.900	21.800	21.900					Swirling
8	45.500	45.300	1.664	1.661	22.800	44.400	44.400	21.600	21.600					Swirling
9	51.600	51.600	1.772	1.772	25.700	47.500	47.400	21.800	21.700					Swirling
10	60.300	59.600	1.916	1.905	29.500	51.700	51.100	22.200	21.600					Swirling
11	70.400	70.400	2.070	2.070	33.900	56.000	55.800	22.100	21.900					Swirling
12	80.800	79.800	2.218	2.204	38.600	60.800	60.400	22.200	21.800					Swirling
13	91.200	90.800	2.356	2.351	44.100	65.800	65.000	21.700	20.900					Swirling
14	99.000	98.500	2.455	2.449	47.700	69.800	68.800	22.100	21.100					Swirling
15	110.100	110.200	2.589	2.590	52.300	74.700	74.600	22.400	22.300					Swirling
16	119.400	-	2.696	-	56.600	78.900	-	22.300	-					Entrain

Shape: Spherical   Size: d=2.7mm   Mass: 1500g   Inclination: 10deg   Overlap: 18deg

Data No.	ΔP across orifice		Superfical Velocity		ΔP across distributor	ΔP across distributor with particle		ΔP across bed		Slugging Time				Observation
	Forward	Reverse	Forward	Reverse		Forward	Reverse	Forward	Reverse	T1	T2	T3	Tavg	
	mmH_2O	*mmH_2O*	*m/sec*	*m/sec*	*mmH_2O*	*mmH_2O*	*mmH_2O*	*mmH_2O*	*mmH_2O*	*s*	*s*	*s*	*s*	
1	12.800	12.700	0.883	16.716	7.000	39.500	36.400	32.500	29.400					Incipient
2	19.000	18.800	1.075	30.107	10.100	42.600	42.300	32.500	32.200					Bubbling
3	22.000	22.000	1.157	38.113	11.600	44.100	43.700	32.500	32.100					Bubbling
4	27.700	27.400	1.299	52.974	14.300	46.500	45.900	32.200	31.600					Bubbling
5	34.200	34.200	1.443	73.871	17.700	49.200	48.900	31.500	31.200					Swirling
6	39.900	39.500	1.558	91.692	20.000	51.700	51.400	31.700	31.400					Swirling
7	45.400	45.600	1.662	113.732	22.800	54.600	54.100	31.800	31.300					Swirling
8	51.100	51.700	1.764	137.301	25.700	58.300	56.900	32.600	31.200					Swirling
9	60.300	60.400	1.916	173.377	29.500	61.900	60.600	32.400	31.100					Swirling
10	70.800	70.300	2.076	217.705	33.900	66.300	65.900	32.400	32.000					Swirling
11	80.200	80.200	2.210	265.276	38.600	69.900	69.400	31.300	30.800					Swirling
12	91.600	91.600	2.361	323.802	44.100	75.000	75.000	30.900	30.900					Swirling
13	99.400	99.000	2.460	363.822	47.700	78.800	78.400	31.100	30.700					Swirling
14	110.200	109.900	2.590	425.533	52.300	83.800	83.400	31.500	31.100					Swirling
15	119.900	-	2.702	-	56.600	88.200	-	31.600	-					Entrain

Shape: Spherical   Size: d=2.7mm   Mass: 2000g   Inclination: 10deg   Overlap: 18deg

Data No.	ΔP across orifice		Superfical Velocity		ΔP across distributor	ΔP across distributor with particle		ΔP across bed		Slugging Time				Observation
	Forward	Reverse	Forward	Reverse		Forward	Reverse	Forward	Reverse	T1	T2	T3	Tavg	
	mmH_2O	*mmH_2O*	*m/sec*	*m/sec*	*mmH_2O*	*mmH_2O*	*mmH_2O*	*mmH_2O*	*mmH_2O*	*s*	*s*	*s*	*s*	
1	15.200	14.800	0.962	0.949	8.500	48.800	48.000	40.300	39.500					Incipient
2	19.000	19.300	1.075	1.084	10.100	51.100	51.300	41.000	41.200					Bubbling
3	24.700	24.100	1.226	1.211	12.800	53.300	52.900	40.500	40.100					Bubbling
4	30.200	29.500	1.356	1.340	15.800	55.500	55.100	39.700	39.300					Bubbling
5	35.300	34.900	1.466	1.458	17.700	57.700	57.500	40.000	39.800					Bubbling
6	39.600	39.600	1.553	1.553	20.000	59.700	59.500	39.700	39.500					Swirling
7	45.600	45.900	1.666	1.672	22.800	62.300	62.400	39.500	39.600					Swirling
8	51.900	51.600	1.777	1.772	25.700	65.500	65.100	39.800	39.400					Swirling
9	60.500	60.100	1.919	1.913	29.500	69.100	68.800	39.600	39.300					Swirling
10	70.800	70.800	2.076	2.076	33.900	73.500	73.500	39.600	39.600					Swirling
11	79.600	80.000	2.201	2.207	38.600	77.600	77.600	39.000	39.000					Swirling
12	91.800	91.500	2.364	2.360	44.100	83.200	83.000	39.100	38.900					Swirling
13	100.000	99.400	2.467	2.460	47.700	86.800	86.200	39.100	38.500					Swirling
14	109.000	-	2.576	-	52.300	91.000	-	38.700	-					Entrain

Shape: Spherical Size: d=3.9mm Mass: 500g Inclination: 10deg Overlap: 18deg

Data No.	ΔP across orifice		Superfical Velocity		ΔP across distributor	ΔP across distributor with particle		ΔP across bed		Slugging Time					Observation
	Forward	Reverse	Forward	Reverse		Forward	Reverse	Forward	Reverse	T1	T2	T3	T4	Tavg	
	mmH_2O	*mmH_2O*	*m/sec*	*m/sec*	*mmH_2O*	*mmH_2O*	*mmH_2O*	*mmH_2O*	*mmH_2O*	*s*	*s*	*s*	*s*	*s*	
1	15.000	14.900	0.956	0.952	9.000	19.800	18.900	10.800	9.900						Incipient
2	17.700	18.100	1.038	1.050	10.500	21.200	21.500	10.700	11.000						Start bubbling
3	20.700	21.000	1.123	1.131	12.100	22.700	22.900	10.600	10.800	1.100	1.030	1.080	0..98	1.070	Slugging
4	23.800	23.900	1.204	1.206	13.600	24.600	24.400	11.000	10.800	1.310	1.360	1.280	1.260	1.303	Slugging
5	26.900	26.900	1.280	1.280	15.200	26.400	26.100	11.200	10.900	1.720	1.620	1.700	1.600	1.660	Slugging
6	29.900	30.000	1.349	1.351	16.600	27.800	27.800	11.200	11.200	1.850	1.820	1.820	1.860	1.838	Slugging
7	35.100	35.000	1.462	1.460	19.200	30.300	30.300	11.100	11.100	2.430	2.310	2.340	2.450	2.383	Slugging
8	40.300	40.300	1.566	1.566	21.700	33.000	32.900	11.300	11.200	2.610	2.670	2.590	2.670	2.635	Slugging
9	45.100	44.900	1.657	1.653	24.200	35.400	35.100	11.200	10.900	3.110	3.720	3.100	3.280	3.303	Slugging
10	49.800	50.400	1.741	1.752	26.700	37.600	38.000	10.900	11.300	Minor slugging					Slugging
11	55.400	55.000	1.836	1.830	29.200	40.600	40.400	11.400	11.200						Swilring
12	60.200	59.800	1.914	1.908	31.600	43.000	42.800	11.400	11.200						Swilring
13	67.600	67.400	2.029	2.026	35.200	46.500	46.400	11.300	11.200						Swilring
14	74.900	75.200	2.135	2.140	38.900	50.200	50.400	11.300	11.500						Swilring
15	82.800	82.900	2.245	2.246	42.400	54.500	54.600	12.100	12.200						Swilring
16	89.700	90.000	2.337	2.341	46.200	58.200	58.000	12.000	11.800						Swilring
17	100.300	100.200	2.471	2.470	51.000	63.600	63.500	12.600	12.500						Swilring
18	110.000	110.200	2.588	2.590	55.900	68.400	68.700	12.500	12.800						Swilring
19	124.900	125.500	2.757	2.764	63.000	76.600	76.600	13.600	13.600						Swilring
20	139.700	139.800	2.916	2.917	70.000	83.900	83.800	13.900	13.800						Swilring
21	155.000	-	3.072	-	77.000	91.000	-	14.000	-						Entrain

Shape: Spherical Size: d=3.9mm Mass: 1000g Inclination: 10deg Overlap: 18deg

Data No.	ΔP across orifice		Superfical Velocity		ΔP across distributor	ΔP across distributor with particle		ΔP across bed		Slugging Time					Observation
	Forward	Reverse	Forward	Reverse		Forward	Reverse	Forward	Reverse	T1	T2	T3	T4	Tavg	
	mmH_2O	*mmH_2O*	*m/sec*	*m/sec*	*mmH_2O*	*mmH_2O*	*mmH_2O*	*mmH_2O*	*mmH_2O*	*s*	*s*	*s*	*s*	*s*	
1	18.000	18.000	1.047	1.047	10.500	32.500	31.600	22.000	21.100						Incipient
2	21.000	21.400	1.131	1.141	12.100	34.500	34.500	22.400	22.400						Start bubbling
3	24.000	23.700	1.209	1.201	13.600	36.100	35.700	22.500	22.100						Start bubbling
4	26.600	26.800	1.272	1.277	15.200	37.100	37.200	21.900	22.000						Bubbling
5	30.000	30.000	1.351	1.351	16.600	39.000	38.800	22.400	22.200						Bubbling
6	35.000	34.600	1.460	1.451	19.200	41.300	41.100	22.100	21.900						Bubbling
7	39.800	40.300	1.557	1.566	21.700	43.700	44.000	22.000	22.300						Bubbling + Swirling
8	44.800	45.300	1.651	1.661	24.200	46.000	46.500	21.800	22.300						Bubbling + Swirling
9	50.300	50.300	1.750	1.750	26.700	48.700	49.000	22.000	22.300						Bubbling + Swirling
10	54.900	55.300	1.828	1.835	29.200	51.600	51.600	22.400	22.400						Bubbling + Swirling
11	60.000	60.100	1.911	1.913	31.600	53.600	53.800	22.000	22.200						Bubbling + Swirling
12	67.800	67.500	2.032	2.027	35.200	57.300	57.500	22.100	22.300						Bubbling + Swirling
13	75.300	75.000	2.141	2.137	38.900	61.200	61.300	22.300	22.400						Swirling
14	82.500	82.800	2.241	2.245	42.400	65.000	65.400	22.600	23.000						Swirling
15	89.800	90.300	2.338	2.345	46.200	68.700	69.300	22.500	23.100						Swirling
16	99.800	100.000	2.465	2.467	51.000	73.900	74.300	22.900	23.300						Swirling
17	109.700	110.100	2.584	2.589	55.900	78.900	79.400	23.000	23.500						Swirling
18	125.000	124.700	2.758	2.755	63.000	86.900	86.900	23.900	23.900						Swirling
19	140.000	139.800	2.919	2.917	70.000	94.500	94.700	24.500	24.700						Swirling
20	155.300	-	3.075	-	77.000	102.900	-	25.900	-						Entrain

Shape: Spherical Size: d=3.9mm Mass: 1500g Inclination: 10deg Overlap: 18deg

Data No.	ΔP across orifice		Superfical Velocity		ΔP across distributor	ΔP across distributor with particle		ΔP across bed		Slugging Time					Observation
	Forward	Reverse	Forward	Reverse		Forward	Reverse	Forward	Reverse	T1	T2	T3	T4	Tavg	
	mmH_2O	mmH_2O	m/sec	m/sec	mmH_2O	mmH_2O	mmH_2O	mmH_2O	mmH_2O	s	s	s	s	s	
1	17.900	18.300	1.044	1.055	10.500	41.500	39.400	31.000	28.900						Incipient
2	21.100	20.800	1.133	1.125	12.100	44.700	43.200	32.600	31.100						Fluidization
3	23.700	24.200	1.201	1.214	13.600	46.000	46.200	32.400	32.600						Start Bubbling
4	26.900	27.200	1.280	1.287	15.200	47.200	47.200	32.000	32.000						Start Bubbling
5	30.000	30.200	1.351	1.356	16.600	48.600	48.800	32.000	32.200						Start Bubbling
6	35.000	35.000	1.460	1.460	19.200	51.000	51.000	31.800	31.800						Bubbling
7	39.900	39.800	1.558	1.557	21.700	53.000	53.200	31.300	31.500						Bubbling
8	45.100	44.900	1.657	1.653	24.200	55.900	55.800	31.700	31.600						Bubbling
9	49.900	49.900	1.743	1.743	26.700	57.900	58.200	31.200	31.500						Bubbling
10	55.200	55.400	1.833	1.836	29.200	60.300	60.500	31.100	31.300						Bubbling+ Swrling
11	60.000	60.300	1.911	1.916	31.600	62.600	63.000	31.000	31.400						Bubbling+ Swrling
12	67.700	67.800	2.030	2.032	35.200	66.500	66.500	31.300	31.300						Bubbling+ Swrling
13	74.700	74.900	2.132	2.135	38.900	70.000	70.100	31.100	31.200						Bubbling+ Swrling
14	82.500	82.500	2.241	2.241	42.400	74.200	74.000	31.800	31.600						Bubbling+ Swrling
15	90.300	90.300	2.345	2.345	46.200	77.700	77.800	31.500	31.600						Bubbling+ Swrling
16	100.000	99.800	2.467	2.465	51.000	82.700	82.600	31.700	31.600						Bubbling+ Swrling
17	110.200	110.000	2.590	2.588	55.900	88.400	88.400	32.500	32.500						Bubbling+ Swrling
18	124.700	125.300	2.755	2.762	63.000	95.900	96.000	32.900	33.000						Jumping
19	140.200	140.000	2.921	2.919	70.000	103.600	103.300	33.600	33.300						Jumping
20	155.000	-	3.072	-	77.000	111.300	-	34.300	-						Jumping

Shape: Spherical Size: d=3.9mm Mass: 2000g Inclination: 10deg Overlap: 18deg

Data No.	ΔP across orifice		Superfical Velocity		ΔP across distributor	ΔP across distributor with particle		ΔP across bed		Slugging Time					Observation
	Forward	Reverse	Forward	Reverse		Forward	Reverse	Forward	Reverse	T1	T2	T3	T4	Tavg	
	mmH_2O	mmH_2O	m/sec	m/sec	mmH_2O	mmH_2O	mmH_2O	mmH_2O	mmH_2O	s	s	s	s	s	
1	20.800	21.300	1.125	1.139	12.100	54.800	50.000	42.700	37.900						Incipient
2	24.200	23.800	1.214	1.204	13.600	59.100	53.800	45.500	40.200						Fluidization
3	26.700	26.900	1.275	1.280	15.200	56.500	55.400	41.300	40.200						Start bubbling
4	29.800	29.700	1.347	1.345	16.600	57.900	57.800	41.300	41.200						Start bubbling
5	35.300	35.100	1.466	1.462	19.200	60.300	60.200	41.100	41.000						Start bubbling
6	40.100	39.800	1.562	1.557	21.700	62.500	62.300	40.800	40.600						Bubbling
7	45.000	45.300	1.655	1.661	24.200	64.900	64.800	40.700	40.600						Bubbling
8	49.700	49.800	1.739	1.741	26.700	67.200	67.000	40.500	40.300						Bubbling
9	55.400	55.400	1.836	1.836	29.200	69.600	69.500	40.400	40.300						Bubbling
10	60.000	60.000	1.911	1.911	31.600	71.700	71.700	40.100	40.100						Bubbling
11	67.800	67.500	2.032	2.027	35.200	75.700	75.300	40.500	40.100						Bottom swirling
12	75.400	75.200	2.142	2.140	38.900	79.200	79.100	40.300	40.200						Bottom swirling
13	82.600	82.300	2.242	2.238	42.400	83.200	82.400	40.800	40.000						Bubbling + Swirling
14	89.700	89.800	2.337	2.338	46.200	86.400	86.100	40.200	39.900						Bubbling + Swirling
15	99.700	99.800	2.464	2.465	51.000	91.800	91.400	40.800	40.400						Bubbling + Swirling
16	110.100	110.200	2.589	2.590	55.900	97.000	96.700	41.100	40.800						Bubbling + Swirling
17	125.000	125.300	2.758	2.762	63.000	104.400	104.300	41.400	41.300						Jumping
18	139.900	140.200	2.918	2.921	70.000	111.900	111.900	41.900	41.900						Jumping
19	155.200	-	3.074	-	77.000	124.500	-	47.500	-						Jumping

Shape: Irregular Size: L/D=1.36 Mass: 500g Inclination: 10deg Overlap: 18deg

Data No.	ΔP across orifice		Superfical Velocity		ΔP across distributor	ΔP across distributor with particle		ΔP across bed		Slugging Time					Observation
	Forward	Reverse	Forward	Reverse		Forward	Reverse	Forward	Reverse	T1	T2	T3	T4	Tavg	
	mmH_2O	mmH_2O	m/sec	m/sec	mmH_2O	mmH_2O	mmH_2O	mmH_2O	mmH_2O	s	s	s	s	s	
1	9.800	10.200	0.772	0.788	5.700	16.400	16.100	10.700	10.400						Incipient
2	12.900	13.100	0.886	0.893	7.400	18.500	18.300	11.100	10.900						Bubbling
3	15.900	16.100	0.984	0.990	8.900	20.300	20.100	11.400	11.200						Bubbling
4	18.800	19.000	1.070	1.075	10.400	21.800	21.800	11.400	11.400	1.530	1.450	1.410	1.400	1.448	Slugging
5	21.900	22.000	1.155	1.157	11.800	23.500	23.600	11.700	11.800	1.820	1.780	1.830	1.730	1.790	Slugging
6	24.900	25.000	1.231	1.234	13.400	24.900	25.000	11.500	11.600	1.910	1.910	1.890	1.880	1.898	Slugging
7	30.000	30.500	1.351	1.363	15.800	27.500	27.800	11.700	12.000	2.400	2.410	2.410	2.420	2.410	Slugging
8	35.000	34.900	1.460	1.458	18.000	29.900	29.700	11.900	11.700	2.670	2.780	2.700	2.740	2.723	Slugging
9	39.800	39.900	1.557	1.558	20.400	31.700	31.800	11.300	11.400						Swirling
10	45.200	45.300	1.659	1.661	22.700	34.000	34.100	11.300	11.400						Swirling
11	50.000	49.800	1.745	1.741	25.000	36.400	36.200	11.400	11.200						Swirling
12	55.300	55.500	1.835	1.838	27.300	39.000	38.900	11.700	11.600						Swirling
13	60.200	60.500	1.914	1.919	29.600	41.400	41.300	11.800	11.700						Swirling
14	69.900	69.600	2.063	2.058	34.000	46.000	46.000	12.000	12.000						Swirling
15	79.900	79.900	2.205	2.205	38.300	51.000	51.400	12.700	13.100						Swirling
16	90.000	90.400	2.341	2.346	43.000	55.600	56.300	12.600	13.300						Swirling
17	99.600	100.200	2.462	2.470	47.600	60.300	61.000	12.700	13.400						Swirling
18	110.300	110.500	2.591	2.594	51.600	65.700	65.700	14.100	14.100						Swirling
19	120.200	-	2.705	-	56.500	70.600	-	14.100	-						Entrain

Shape: Irregular Size: L/D=1.36 Mass: 1000g Inclination: 10deg Overlap: 18deg

Data No.	ΔP across orifice		Superfical Velocity		ΔP across distributor	ΔP across distributor with particle		ΔP across bed		Slugging Time					Observation
	Forward	Reverse	Forward	Reverse		Forward	Reverse	Forward	Reverse	T1	T2	T3	T4	Tavg	
	mmH_2O	mmH_2O	m/sec	m/sec	mmH_2O	mmH_2O	mmH_2O	mmH_2O	mmH_2O	s	s	s	s	s	
1	12.900	13.100	0.886	0.893	7.400	29.000	27.900	21.600	20.500						Incipient
2	15.900	16.100	0.984	0.990	8.900	30.900	29.900	22.000	21.000						Bubbling
3	19.200	19.500	1.081	1.090	10.400	32.700	32.000	22.300	21.600						Bubbling
4	22.000	22.400	1.157	1.168	11.800	34.100	33.300	22.300	21.500						Bubbling
5	25.100	24.800	1.236	1.229	13.400	35.500	34.500	22.100	21.100						Bubbling
6	29.800	30.100	1.347	1.354	15.800	37.800	36.700	22.000	20.900						Slow Swirling
7	34.900	34.500	1.458	1.449	18.000	40.100	38.700	22.100	20.700						Swirling
8	40.000	40.100	1.560	1.562	20.400	42.400	41.100	22.000	20.700						Swirling
9	45.000	44.600	1.655	1.648	22.700	44.100	43.200	21.400	20.500						Swirling
10	50.400	49.700	1.752	1.739	25.000	46.600	45.700	21.600	20.700						Swirling
11	55.000	54.700	1.830	1.825	27.300	48.600	48.200	21.300	20.900						Swirling
12	59.800	59.700	1.908	1.906	29.600	50.500	50.700	20.900	21.100						Swirling
13	64.700	64.900	1.985	1.988	31.700	53.300	53.400	21.600	21.700						Swirling
14	70.300	70.000	2.069	2.064	34.000	56.100	56.000	22.100	22.000						Swirling
15	79.900	80.000	2.205	2.207	38.300	61.200	61.200	22.900	22.900						Swirling
16	90.000	90.000	2.341	2.341	43.000	66.300	66.200	23.300	23.200						Swirling
17	99.800	100.400	2.465	2.472	47.600	71.300	71.400	23.700	23.800						Jumping
18	109.800	-	2.585	-	51.600	76.400	-	24.800	-						Entrain

Shape: Irregular Size: L/D=1.36 Mass: 1500g Inclination: 10deg Overlap: 18deg

Data No.	ΔP across orifice		Superfical Velocity		ΔP across distributor	ΔP across distributor with particle		ΔP across bed		Slugging Time					Observation
	Forward	Reverse	Forward	Reverse		Forward	Reverse	Forward	Reverse	T1	T2	T3	T4	Tavg	
	mmH_2O	mmH_2O	m/sec	m/sec	mmH_2O	mmH_2O	mmH_2O	mmH_2O	mmH_2O	s	s	s	s	s	
1	13.000	12.900	0.890	0.886	7.400	38.900	36.800	31.500	29.400						Incipient
2	15.800	16.000	0.981	0.987	8.900	40.400	38.400	31.500	29.500						Bubbling
3	18.700	18.700	1.067	1.067	10.400	41.600	39.800	31.200	29.400						Bubbling
4	22.000	22.100	1.157	1.160	11.800	43.000	41.500	31.200	29.700						Bubbling
5	25.100	25.100	1.236	1.236	13.400	44.300	42.800	30.900	29.400						Bottom swirling
6	30.200	30.200	1.356	1.356	15.800	46.800	45.000	31.000	29.200						Bottom swirling
7	34.900	34.800	1.458	1.455	18.000	48.700	46.900	30.700	28.900						Bottom swirling
8	39.800	40.000	1.557	1.560	20.400	50.700	49.200	30.300	28.800						Bottom swirling
9	44.600	44.700	1.648	1.650	22.700	53.100	51.400	30.400	28.700						Bottom swirling
10	49.800	50.300	1.741	1.750	25.000	55.500	54.400	30.500	29.400						Bottom swirling
11	55.200	55.200	1.833	1.833	27.300	57.700	56.600	30.400	29.300						Bottom swirling
12	60.000	60.300	1.911	1.916	29.600	60.000	59.200	30.400	29.600						Bottom swirling
13	70.000	69.900	2.064	2.063	34.000	64.700	64.400	30.700	30.400						Bottom swirling
14	79.600	80.000	2.201	2.207	38.300	69.500	69.400	31.200	31.100						Entrain
15	90.200	90.400	2.343	2.346	43.000	75.000	74.900	32.000	31.900						Entrain
16	99.800	-	2.465	-	47.600	79.900	-	32.300	-						Entrain

Shape: Irregular Size: L/D=1.36 Mass: 2000g Inclination: 10deg Overlap: 18deg

Data No.	ΔP across orifice		Superfical Velocity		ΔP across distributor	ΔP across distributor with particle		ΔP across bed		Slugging Time					Observation
	Forward	Reverse	Forward	Reverse		Forward	Reverse	Forward	Reverse	T1	T2	T3	T4	Tavg	
	mmH_2O	mmH_2O	m/sec	m/sec	mmH_2O	mmH_2O	mmH_2O	mmH_2O	mmH_2O	s	s	s	s	s	
1	12.800	12.700	0.883	0.879	7.400	46.300	44.000	38.900	36.600						Incipient
2	16.300	16.300	0.996	0.996	8.900	48.500	47.100	39.600	38.200						Bubbling
3	19.100	19.200	1.078	1.081	10.400	49.800	48.800	39.400	38.400						Bubbling
4	22.000	22.000	1.157	1.157	11.800	51.300	50.100	39.500	38.300						Bubbling
5	25.200	25.400	1.239	1.243	13.400	52.500	51.500	39.100	38.100						Bubbling
6	30.200	29.800	1.356	1.347	15.800	54.900	53.400	39.100	37.600						Bubbling
7	34.700	34.700	1.453	1.453	18.000	57.000	55.700	39.000	37.700						Two-layer
8	39.600	40.200	1.553	1.564	20.400	58.700	58.300	38.300	37.900						Two-layer
9	44.700	45.400	1.650	1.662	22.700	61.100	61.000	38.400	38.300						Two-layer
10	49.800	49.800	1.741	1.741	25.000	63.200	63.000	38.200	38.000						Two-layer
11	54.900	55.000	1.828	1.830	27.300	65.700	65.500	38.400	38.200						Two-layer
12	60.400	60.000	1.917	1.911	29.600	68.100	67.400	38.500	37.800						Two-layer
13	64.800	65.300	1.986	1.994	31.700	70.500	70.100	38.800	38.400						Two-layer
14	70.200	70.000	2.067	2.064	34.000	72.900	72.500	38.900	38.500						Two-layer
15	80.100	80.300	2.208	2.211	38.300	77.500	77.200	39.200	38.900						Jumping
16	89.900	-	2.339	-	43.000	82.700	-	39.700	-						Entrain

Shape: Irregular Size: L/D=2.00 Mass: 500g Inclination: 10deg Overlap: 18deg

Data No.	ΔP across orifice		Superfical Velocity		ΔP across distributor	ΔP across distributor with particle		ΔP across bed		Slugging Time					Observation
	Forward	Reverse	Forward	Reverse		Forward	Reverse	Forward	Reverse	T1	T2	T3	T4	Tavg	
	mmH_2O	*mmH_2O*	*m/sec*	*m/sec*	*mmH_2O*	*mmH_2O*	*mmH_2O*	*mmH_2O*	*mmH_2O*	*s*	*s*	*s*	*s*	*s*	
1	12.900	13.300	0.886	0.900	8.100	16.700	17.800	8.600	9.700						Incipient
2	15.800	15.900	0.981	0.984	9.600	20.700	20.500	11.100	10.900						Start swirling
3	19.000	18.900	1.075	1.073	11.300	22.300	22.300	11.000	11.000	1.040	0.980	0.980	0.890	0.973	Slugging
4	21.800	22.200	1.152	1.162	12.900	23.500	23.700	10.600	10.800	1.540	1.530	1.680	1.570	1.580	Slugging
5	25.000	24.800	1.234	1.229	14.500	25.200	25.200	10.700	10.700	1.840	1.800	1.730	1.880	1.813	Slugging
6	29.800	30.000	1.347	1.351	16.900	28.000	28.000	11.100	11.100	2.330	2.400	2.240	2.320	2.323	Slugging
7	34.900	35.300	1.458	1.466	19.300	30.800	30.900	11.500	11.600	2.520	2.600	2.530	2.520	2.543	Slugging
8	39.800	40.200	1.557	1.564	22.000	33.800	33.800	11.800	11.800	2.580	2.660	2.640	2.640	2.630	Slugging
9	45.300	45.400	1.661	1.662	24.300	36.000	36.200	11.700	11.900						Swirling
10	50.100	50.400	1.746	1.752	26.900	38.500	39.000	11.600	12.100						Swirling
11	55.200	55.200	1.833	1.833	29.500	41.100	41.600	11.600	12.100						Swirling
12	60.000	59.900	1.911	1.910	31.500	44.500	44.200	13.000	12.700						Swirling
13	67.500	67.500	2.027	2.027	35.500	48.300	48.100	12.800	12.600						Swirling
14	74.900	74.900	2.135	2.135	39.000	51.600	51.700	12.600	12.700						Swirling
15	82.500	82.400	2.241	2.240	43.100	55.600	55.600	12.500	12.500						Swirling
16	90.000	89.900	2.341	2.339	46.000	57.800	60.000	11.800	14.000						Swirling
17	100.200	100.300	2.470	2.471	51.000	65.400	65.600	14.400	14.600						Jumping
18	109.800	109.900	2.585	2.586	56.100	70.600	70.500	14.500	14.400						Jumping
19	120.000	-	2.703	-	61.100	75.100	-	14.000	-						Entrain

Shape: Irregular Size: L/D=2.00 Mass: 1000g Inclination: 10deg Overlap: 18deg

Data No.	ΔP across orifice		Superfical Velocity		ΔP across distributor	ΔP across distributor with particle		ΔP across bed		Slugging Time					Observation
	Forward	Reverse	Forward	Reverse		Forward	Reverse	Forward	Reverse	T1	T2	T3	T4	Tavg	
	mmH_2O	*mmH_2O*	*m/sec*	*m/sec*	*mmH_2O*	*mmH_2O*	*mmH_2O*	*mmH_2O*	*mmH_2O*	*s*	*s*	*s*	*s*	*s*	
1	19.200	18.800	1.081	1.070	11.300	33.400	31.700	22.100	20.400						Incipient
2	21.800	22.300	1.152	1.165	12.900	34.500	34.700	21.600	21.800						Start bubbling
3	25.200	25.200	1.239	1.239	14.500	36.000	36.000	21.500	21.500						Bubbling
4	29.900	30.000	1.349	1.351	16.900	38.700	38.600	21.800	21.700						Bubbling
5	35.300	35.400	1.466	1.468	19.300	41.600	41.300	22.300	22.000						Bubbling
6	39.600	39.800	1.553	1.557	22.000	43.900	43.200	21.900	21.200	1.450	2.680	2.600	2.680	2.353	Slugging
7	44.900	45.100	1.653	1.657	24.300	46.700	46.500	22.400	22.200	1.440	2.980	2.970	2.890	2.570	Slugging
8	50.000	50.200	1.745	1.748	26.900	48.700	48.600	21.800	21.700	1.640	3.010	3.110	3.140	2.725	Slugging
9	55.000	55.300	1.830	1.835	29.500	51.100	51.300	21.600	21.800	1.640	3.170	3.230	3.090	2.783	Slugging
10	60.100	59.800	1.913	1.908	31.500	53.700	53.500	22.200	22.000	Minor Slugging					Slugging
11	67.300	67.600	2.024	2.029	35.500	57.900	57.900	22.400	22.400						Swirling
12	75.300	75.300	2.141	2.141	39.000	62.400	61.900	23.400	22.900						Swirling
13	82.700	82.500	2.244	2.241	43.100	66.500	65.800	23.400	22.700						Swirling
14	89.900	89.800	2.339	2.338	46.000	69.200	69.200	23.200	23.200						Swirling
15	100.300	100.000	2.471	2.467	51.000	75.000	74.800	24.000	23.800						Swirling
16	109.800	109.900	2.585	2.586	56.100	79.700	79.700	23.600	23.600						Jumping
17	120.000	120.000	2.703	2.703	61.100	84.800	84.800	23.700	23.700						Jumping
18	129.800	-	2.811	-	65.600	89.200	-	23.600	-						Entrain

Shape: Irregular Size: L/D=2.00 Mass: 1500g Inclination: 10deg Overlap: 18deg

Data No.	ΔP across orifice		Superfical Velocity		ΔP across distributor	ΔP across distributor with particle		ΔP across bed		Slugging Time				Observation
	Forward	Reverse	Forward	Reverse		Forward	Reverse	Forward	Reverse	T1	T2	T3	Tavg	
	mmH_2O	*mmH_2O*	*m/sec*	*m/sec*	*mmH_2O*	*mmH_2O*	*mmH_2O*	*mmH_2O*	*mmH_2O*	*s*	*s*	*s*	*s*	
1	18.900	19.100	1.073	1.078	11.300	43.700	38.900	32.400	27.600					Fluidized
2	22.200	22.200	1.162	1.162	12.900	44.500	42.000	31.600	29.100					Start bubbling
3	24.900	24.600	1.231	1.224	14.500	45.600	45.000	31.100	30.500					Bubbling
4	29.900	29.900	1.349	1.349	16.900	47.700	47.400	30.800	30.500					Bubbling
5	35.000	35.000	1.460	1.460	19.300	50.000	50.300	30.700	31.000					Bubbling
6	39.900	40.200	1.558	1.564	22.000	52.500	51.900	30.500	29.900					Slugging
7	45.300	45.300	1.661	1.661	24.300	55.100	54.600	30.800	30.300					Bottom swirling
8	49.800	50.200	1.741	1.748	26.900	57.500	56.900	30.600	30.000					Bottom swirling
9	54.900	55.300	1.828	1.835	29.500	60.200	59.700	30.700	30.200					Bottom swirling
10	60.000	60.200	1.911	1.914	31.500	62.800	62.700	31.300	31.200					Bottom swirling
11	67.400	67.400	2.026	2.026	35.500	66.400	66.300	30.900	30.800					Jumping
12	75.000	75.000	2.137	2.137	39.000	70.900	70.500	31.900	31.500					Jumping
13	82.500	82.500	2.241	2.241	43.100	74.600	74.300	31.500	31.200					Jumping
14	90.400	90.400	2.346	2.346	46.000	78.500	78.000	32.500	32.000					Jumping
15	100.300	100.300	2.471	2.471	51.000	83.200	83.000	32.200	32.000					Jumping
16	110.000	110.200	2.588	2.590	56.100	89.300	88.400	33.200	32.300					Jumping
17	120.300	-	2.706	-	61.100	93.400	-	32.300	-					Jumping

Shape: Irregular Size: L/D=2.00 Mass: 2000g Inclination: 10deg Overlap: 18deg

Data No.	ΔP across orifice		Superfical Velocity		ΔP across distributor	ΔP across distributor with particle		ΔP across bed		Slugging Time				Observation
	Forward	Reverse	Forward	Reverse		Forward	Reverse	Forward	Reverse	T1	T2	T3	Tavg	
	mmH_2O	*mmH_2O*	*m/sec*	*m/sec*	*mmH_2O*	*mmH_2O*	*mmH_2O*	*mmH_2O*	*mmH_2O*	*s*	*s*	*s*	*s*	
1	22.300	21.900	1.000	1.018	12.900	51.200	49.000	38.300	36.100					Fluidized
2	24.900	25.000	1.231	1.234	14.500	54.600	54.600	40.100	40.100					Bottom swirling
3	30.000	29.900	1.351	1.349	16.900	56.800	56.800	39.900	39.900					Bottom swirling
4	34.700	35.200	1.453	1.464	19.300	58.800	58.900	39.500	39.600					Bottom swirling
5	39.900	40.300	1.558	1.566	22.000	60.500	59.900	38.500	37.900					Bottom swirling
6	45.000	44.900	1.655	1.653	24.300	62.800	62.000	38.500	37.700					Bottom swirling
7	50.300	50.000	1.750	1.745	26.900	65.700	64.800	38.800	37.900					Bottom swirling
8	55.200	55.300	1.833	1.835	29.500	68.400	68.000	38.900	38.500					Bottom swirling
9	60.200	60.000	1.914	1.911	31.500	70.800	70.200	39.300	38.700					Bottom swirling
10	67.500	67.800	2.027	2.032	35.500	74.700	74.700	39.200	39.200					Bottom swirling
11	75.000	74.900	2.137	2.135	39.000	78.700	78.100	39.700	39.100					Bottom swirling
12	82.500	82.500	2.241	2.241	43.100	82.700	82.100	39.600	39.000					Bottom swirling
13	89.900	90.000	2.339	2.341	46.000	86.000	85.800	40.000	39.800					Bottom swirling
17	100.100	99.800	2.468	2.465	51.000	91.000	90.800	40.000	39.800					Jumping
18	110.000	-	2.588	-	56.100	96.100	-	40.000	-					Jumping

Shape: Cylindrical Size: L/D=1.28 Mass: 500g Inclination: 10deg Overlap: 18deg

Data No.	ΔP across orifice		Superfical Velocity		ΔP across distributor	ΔP across distributor with particle		ΔP across bed		Slugging Time					Observation
	Forward	Reverse	Forward	Reverse		Forward	Reverse	Forward	Reverse	T1	T2	T3	T4	Tavg	
	mmH_2O	mmH_2O	m/sec	m/sec	mmH_2O	mmH_2O	mmH_2O	mmH_2O	mmH_2O	s	s	s	s	s	
1	6.100	6.200	0.609	0.614	4.000	11.600	6.300	7.600	2.300						Incipient
2	8.900	9.300	0.736	0.752	5.700	15.300	9.200	9.600	3.500						Incipient
3	12.300	12.300	0.865	0.865	7.300	17.700	11.600	10.400	4.300						Massing
4	15.300	14.800	0.965	0.949	9.000	17.700	13.600	8.700	4.600						Massing
5	19.800	20.400	1.098	1.114	11.600	18.000	18.300	6.400	6.700						Massing
6	24.900	25.200	1.231	1.239	14.200	24.100	23.700	9.900	9.500						Massing
7	30.000	30.000	1.351	1.351	16.700	27.200	26.900	10.500	10.200	7.140	7.250	7.160	7.210	7.190	Slugging
8	34.800	35.300	1.455	1.466	19.300	29.900	30.200	10.600	10.900	6.220	6.210	6.230	6.220	6.220	Slugging
9	40.100	39.900	1.562	1.558	21.800	32.800	32.600	11.000	10.800	5.640	5.560	5.620	5.590	5.603	Slugging
10	44.800	45.200	1.651	1.659	24.300	35.600	35.600	11.300	11.300	5.530	5.480	5.520	5.530	5.515	Slugging
11	50.200	49.800	1.748	1.741	26.800	38.300	38.000	11.500	11.200	5.120	5.210	5.150	5.170	5.163	Slugging
12	55.400	55.300	1.836	1.835	29.200	41.200	41.200	12.000	12.000						Swirling
13	60.300	60.000	1.916	1.911	31.800	43.900	43.800	12.100	12.000						Swirling
14	65.200	65.000	1.992	1.989	34.100	46.400	46.400	12.300	12.300						Swirling
15	70.000	69.800	2.064	2.061	36.600	49.000	48.800	12.400	12.200						Swirling
16	79.800	80.000	2.204	2.207	41.200	53.900	53.900	12.700	12.700						Swirling
17	89.700	90.300	2.337	2.345	46.400	59.100	59.200	12.700	12.800						Jumping
18	105.000	105.300	2.528	2.532	53.600	66.500	66.800	12.900	13.200						Entrain
19	120.200	-	2.705	-	60.800	74.200	-	13.400							Entrain

Shape: Cylindrical Size: L/D=1.28 Mass: 1000g Inclination: 10deg Overlap: 18deg

Data No.	ΔP across orifice		Superfical Velocity		ΔP across distributor	ΔP across distributor with particle		ΔP across bed		Slugging Time					Observation
	Forward	Reverse	Forward	Reverse		Forward	Reverse	Forward	Reverse	T1	T2	T3	T4	Tavg	
	mmH_2O	mmH_2O	m/sec	m/sec	mmH_2O	mmH_2O	mmH_2O	mmH_2O	mmH_2O	s	s	s	s	s	
1	12.000	12.000	0.855	0.855	7.300	28.400	22.500	21.100	15.200						Incipient
2	15.200	15.000	0.962	0.956	9.000	31.800	26.500	22.800	17.500						Bubbling
3	20.200	20.200	1.109	1.109	11.600	34.600	30.900	23.000	19.300						Bubbling
4	25.000	25.200	1.234	1.239	14.200	35.200	33.900	21.000	19.700						Bubbling
5	30.000	30.000	1.351	1.351	16.700	39.000	38.500	22.300	21.800						Bubbling
6	35.100	35.000	1.462	1.460	19.300	41.900	40.800	22.600	21.500	2.540	2.460	2.420	2.410	2.458	Slugging
7	40.100	40.400	1.562	1.568	21.800	45.000	43.900	23.200	22.100	2.650	2.720	2.750	2.770	2.723	Slugging
8	45.000	44.900	1.655	1.653	24.300	48.000	47.100	23.700	22.800	2.890	2.920	2.950	2.900	2.915	Slugging
9	50.400	50.400	1.752	1.752	26.800	50.600	50.200	23.800	23.400	2.890	3.010	2.950	2.980	2.958	Slugging
10	55.200	55.200	1.833	1.833	29.200	52.600	52.500	23.400	23.300	3.010	3.073	3.000	3.050	3.033	Slugging
11	60.300	360.000	1.916	4.681	31.800	56.000	55.600	24.200	23.800	2.920	2.910	2.920	2.910	2.915	Slugging
12	65.200	65.000	1.992	1.989	34.100	59.700	58.100	25.600	24.000	3.010	2.980	3.020	3.040	3.013	Slugging
13	70.000	70.300	2.064	2.069	36.600	60.800	61.100	24.200	24.500						Swirling
14	79.900	79.800	2.205	2.204	41.200	66.000	65.800	24.800	24.600						Swirling
15	90.000	89.700	2.341	2.337	46.400	70.800	70.200	24.400	23.800						Swirling
16	100.100	99.900	2.468	2.466	51.000	75.400	75.300	24.400	24.300						Swirling
17	110.300	109.900	2.591	2.586	55.700	81.900	81.200	26.200	25.500						Swirling
18	120.200	120.200	2.705	2.705	65.600	86.600	86.300	21.000	20.700						Swirling
19	130.200	129.700	2.815	2.810	65.600	92.000	91.600	26.400	26.000						Jumping
20	139.700	-	2.916	-	70.300	97.200		26.900							Entrain

Shape: Cylindrical Size: L/D=1.28 Mass: 1500g Inclination: 10deg Overlap: 18deg

Data No.	ΔP across orifice		Superfical Velocity		ΔP across distributor	ΔP across distributor with particle		ΔP across bed		Slugging Time					Observation
	Forward	Reverse	Forward	Reverse		Forward	Reverse	Forward	Reverse	T1	T2	T3	T4	Tavg	
	mmH_2O	mmH_2O	m/sec	m/sec	mmH_2O	mmH_2O	mmH_2O	mmH_2O	mmH_2O	s	s	s	s	s	
1	11.800	12.400	0.848	0.869	7.300	31.300	30.700	24.000	23.400						Incipient
2	15.100	15.400	0.959	0.968	9.000	38.300	36.700	29.300	27.700						Incipient
3	20.300	20.100	1.112	1.106	11.600	41.900	41.300	30.300	29.700						Bubbling
4	24.900	25.300	1.231	1.241	14.200	44.900	45.100	30.700	30.900						Bubbling
5	30.100	30.300	1.354	1.358	16.700	48.600	48.800	31.900	32.100						Bubbling
6	35.300	35.400	1.466	1.468	19.300	53.000	52.800	33.700	33.500						Bubbling
7	40.300	39.800	1.566	1.557	21.800	56.100	55.600	34.300	33.800	1.950	1.980	1.910	1.920	1.940	Slugging
8	44.800	44.800	1.651	1.651	24.300	58.700	58.300	34.400	34.000	1.970	1.990	2.010	1.950	1.980	Slugging
9	50.100	50.300	1.746	1.750	26.800	61.300	61.400	34.500	34.600	2.090	2.140	2.170	2.120	2.130	Slugging
10	55.100	55.300	1.831	1.835	29.200	64.600	64.600	35.400	35.400	2.220	2.170	2.200	2.210	2.200	Slugging
11	60.300	60.000	1.916	1.911	31.800	66.700	66.700	34.900	34.900	2.270	2.330	2.340	2.310	2.313	Slugging
12	65.000	65.000	1.989	1.989	34.100	69.400	69.200	35.300	35.100	2.420	2.450	2.350	2.320	2.385	Slugging
13	70.200	70.100	2.067	2.066	36.600	72.900	72.100	36.300	35.500	2.570	2.600	2.560	2.590	2.580	Slugging
14	79.800	80.300	2.204	2.211	41.200	76.900	77.000	35.700	35.800	2.520	2.450	2.470	2.560	2.500	Slugging
15	90.200	90.000	2.343	2.341	46.400	81.600	81.500	35.200	35.100	Minor Slugging					Slugging
16	99.700	99.800	2.464	2.465	51.000	86.600	86.900	35.600	35.900						Jumping
17	114.800	114.700	2.644	2.642	58.200	95.200	94.800	37.000	36.600						Jumping
18	130.100	129.900	2.814	2.812	65.600	102.700	102.500	37.100	36.900						Entrain
19	139.800	-	2.917	-	70.300	108.000	-	37.700	-						Entrain

Shape: Cylindrical Size: L/D=1.28 Mass: 2000g Inclination: 10deg Overlap: 18deg

Data No.	ΔP across orifice		Superfical Velocity		ΔP across distributor	ΔP across distributor with particle		ΔP across bed		Slugging Time					Observation
	Forward	Reverse	Forward	Reverse		Forward	Reverse	Forward	Reverse	T1	T2	T3	T4	Tavg	
	mmH_2O	mmH_2O	m/sec	m/sec	mmH_2O	mmH_2O	mmH_2O	mmH_2O	mmH_2O	s	s	s	s	s	
1	12.200	11.900	0.862	0.851	7.300	40.000	35.200	32.700	27.900						Incipient
2	15.000	14.800	0.956	0.949	9.000	46.100	41.700	37.100	32.700						Incipient
3	20.300	19.900	1.112	1.101	11.600	51.800	49.900	40.200	38.300						Start bubbling
4	24.700	25.100	1.226	1.236	14.200	54.000	53.800	39.800	39.600						Bubbling
5	30.000	30.000	1.351	1.351	16.700	58.000	57.700	41.300	41.000						Bubbling
6	35.200	35.400	1.464	1.468	19.300	62.100	61.700	42.800	42.400						Bubbling
7	39.900	40.200	1.558	1.564	21.800	64.900	64.800	43.100	43.000						Bubbling
8	45.300	45.300	1.661	1.661	24.300	67.700	67.700	43.400	43.400	0.670	0.760	0.640	0.770		Slugging
9	50.400	50.100	1.752	1.746	26.800	71.300	71.000	44.500	44.200	1.650	1.700	1.660	1.670		Slugging
10	54.800	55.000	1.826	1.830	29.200	73.900	74.000	44.700	44.800	1.520	1.580	1.610	1.650		Slugging
11	60.000	60.000	1.911	1.911	31.800	76.500	76.300	44.700	44.500	1.850	1.890	1.850	1.880		Slugging
12	65.300	65.300	1.994	1.994	34.100	78.700	78.700	44.600	44.600	1.830	1.790	1.750	1.740		Slugging
13	69.800	70.200	2.061	2.067	36.600	81.000	81.300	44.400	44.700	Minor slugging					Slugging
14	79.700	80.300	2.203	2.211	41.200	85.800	85.800	44.600	44.600	Minor slugging					Slugging
15	89.800	89.800	2.338	2.338	46.400	91.200	91.000	44.800	44.600						Jumping
16	99.800	100.400	2.465	2.472	51.000	95.800	96.000	44.800	45.000						Jumping
17	115.400	115.000	2.650	2.646	58.200	103.800	103.700	45.600	45.500						Jumping
18	130.000	130.000	2.813	2.813	65.600	111.100	110.900	45.500	45.300						Entrain
19	139.800	-	2.917	-	70.300	116.000	-	45.700							Entrain

Shape: Cylindrical Size: L/D=4.10 Mass: 500g Inclination: 10deg Overlap: 18deg

Data No.	ΔP across orifice		Superfical Velocity		ΔP across distributor	ΔP across distributor with particle		ΔP across bed		Slugging Time					Observation
	Forward	Reverse	Forward	Reverse		Forward	Reverse	Forward	Reverse	T1	T2	T3	T4	Tavg	
	mmH_2O	mmH_2O	m/sec	m/sec	mmH_2O	mmH_2O	mmH_2O	mmH_2O	mmH_2O	s	s	s	s	s	
1	12.300	12.500	0.865	0.872	7.100	16.400	11.000	9.300	3.900						Fluidization
2	14.900	15.000	0.952	0.956	8.300	19.100	13.000	10.800	4.700						Fluidization
3	18.100	18.600	1.050	1.064	9.900	21.200	15.700	11.300	5.800						Fluidization
4	20.900	20.400	1.128	1.114	10.800	23.000	17.000	12.200	6.200						Channeling
5	24.800	24.800	1.229	1.229	12.900	25.000	20.300	12.100	7.400						Channeling
6	29.000	29.400	1.329	1.338	15.100	25.900	23.600	10.800	8.500						Channeling
7	33.800	33.900	1.434	1.437	16.700	27.300	27.000	10.600	10.300						Bubbling
8	38.300	38.700	1.527	1.535	19.000	29.100	29.100	10.100	10.100	7.400	7.860	7.410	7.900	7.643	Slugging
9	42.100	41.600	1.601	1.591	20.700	30.900	30.500	10.200	9.800	8.950	8.830	9.180	8.480	8.860	Slugging
10	45.900	45.900	1.672	1.672	22.300	32.600	32.600	10.300	10.300	7.480	7.480	7.830	7.860	7.663	Slugging
11	49.700	50.300	1.739	1.750	24.000	34.500	34.800	10.500	10.800	7.280	6.900	6.920	7.370	7.118	Slugging
12	55.100	55.600	1.831	1.840	26.500	37.200	37.500	10.700	11.000	6.340	6.400	6.390	6.140	6.318	Slugging
13	59.400	60.400	1.902	1.917	28.200	39.400	39.900	11.200	11.700	6.090	5.780	5.760	5.920	5.888	Slugging
14	65.000	65.400	1.989	1.995	30.600	42.100	42.500	11.500	11.900	5.980	5.910	6.080	5.920	5.973	Slugging
15	70.000	69.600	2.064	2.058	32.600	44.700	44.400	12.100	11.800	5.220	5.350	5.710	5.550	5.458	Slugging
16	75.100	75.300	2.138	2.141	34.700	47.100	47.100	12.400	12.400						Swirling
17	85.000	85.600	2.275	2.283	39.200	51.800	52.000	12.600	12.800						Swirling
18	95.000	95.000	2.405	2.405	43.500	56.300	56.000	12.800	12.500						Swirling
19	105.100	105.100	2.529	2.529	47.900	60.900	60.600	13.000	12.700						Swirling
20	115.400	115.800	2.650	2.655	52.200	65.900	66.800	13.700	14.600						Swirling
21	125.100	125.400	2.760	2.763	56.300	70.000	71.400	13.700	15.100						Swirling
22	134.900	135.300	2.866	2.870	60.500	74.700	75.500	14.200	15.000						Swirling
23	145.000	-	2.971	-	64.900	80.200	80.200	15.300	-						Jumping

Shape: Cylindrical Size: L/D=4.10 Mass: 1000g Inclination: 10deg Overlap: 18deg

Data No.	ΔP across orifice		Superfical Velocity		ΔP across distributor	ΔP across distributor with particle		ΔP across bed		Slugging Time					Observation
	Forward	Reverse	Forward	Reverse		Forward	Reverse	Forward	Reverse	T1	T2	T3	T4	Tavg	
	mmH_2O	mmH_2O	m/sec	m/sec	mmH_2O	mmH_2O	mmH_2O	mmH_2O	mmH_2O	s	s	s	s	s	
1	20.000	20.800	1.103	1.125	10.800	25.100	23.900	14.300	13.100						Fluidization
2	24.600	24.600	1.224	1.224	12.900	29.700	27.200	16.800	14.300						Channeling
3	29.400	29.500	1.338	1.340	15.100	34.500	31.400	19.400	16.300						Channeling
4	33.300	33.400	1.424	1.426	16.700	37.700	34.700	21.000	18.000						Channeling
5	38.800	38.400	1.537	1.529	19.000	41.300	38.800	22.300	19.800						Bubbling
6	42.500	41.800	1.608	1.595	20.700	42.600	41.400	21.900	20.700						Bubbling
7	46.400	46.500	1.681	1.682	22.300	43.700	44.100	21.400	21.800	1.230	1.210	1.280	1.350	1.268	Slugging
8	49.500	49.500	1.736	1.736	24.000	44.600	44.800	20.600	20.800	1.980	1.660	1.670	1.960	1.818	Slugging
9	55.100	55.100	1.831	1.831	26.500	47.900	47.800	21.400	21.300	2.040	2.090	2.200	2.230	2.140	Slugging
10	59.800	60.200	1.908	1.914	28.200	50.700	50.600	22.500	22.400	2.350	2.280	2.270	2.420	2.330	Slugging
11	65.200	65.600	1.992	1.998	30.600	53.500	53.600	22.900	23.000	2.550	2.890	2.480	2.690	2.653	Slugging
12	70.200	70.100	2.067	2.066	32.600	56.000	55.800	23.400	23.200	2.540	2.460	4.610	2.410	3.005	Slugging
13	74.800	75.200	2.134	2.140	34.700	58.200	58.300	23.500	23.600	2.640	2.730	2.600	2.560	2.633	Slugging
14	84.500	84.400	2.268	2.267	39.200	63.200	63.000	24.000	23.800	2.950	2.790	2.830	2.920	2.873	Slugging
15	95.200	94.800	2.407	2.402	43.500	68.100	68.000	24.600	24.500	2.910	2.890	2.820	2.860	2.870	Slugging
16	105.100	105.700	2.529	2.537	47.900	73.100	73.700	25.200	25.800						Swirling
17	115.500	115.100	2.652	2.647	52.200	77.600	77.800	25.400	25.600						Swirling
18	125.000	125.100	2.758	2.760	56.300	82.200	82.300	25.900	26.000						Swirling
19	135.000	135.000	2.867	2.867	60.500	86.300	86.400	25.800	25.900						Swirling
20	144.500	-	2.966	-	64.900	90.800	-	25.900	-						Swirling

* Hysteresis effect is obvious at channeling period

Shape: Cylindrical Size: L/D=4.10 Mass: 1500g Inclination: 10deg Overlap: 18deg

Data No.	ΔP across orifice		Superfical Velocity		ΔP across distributor	ΔP across distributor with particle		ΔP across bed		Slugging Time					Observation
	Forward	Reverse	Forward	Reverse		Forward	Reverse	Forward	Reverse	T1	T2	T3	T4	Tavg	
	mmH_2O	mmH_2O	m/sec	m/sec	mmH_2O	mmH_2O	mmH_2O	mmH_2O	mmH_2O	s	s	s	s	s	
1	25.200	25.100	1.239	1.236	12.900	41.000	33.900	28.100	21.000						Fluidization
2	29.000	28.300	1.329	1.313	15.100	46.000	37.200	30.900	22.100						Channeling
3	33.000	33.200	1.417	1.422	16.700	49.400	42.200	32.700	25.500						Channeling
4	38.000	38.400	1.521	1.529	19.000	50.100	47.600	31.100	28.600						Channeling
5	42.500	42.800	1.608	1.614	20.700	52.600	51.600	31.900	30.900						Channeling
6	46.200	46.100	1.677	1.675	22.300	55.100	54.100	32.800	31.800						Bubbling
7	50.000	49.300	1.745	1.732	24.000	57.200	56.000	33.200	32.000						Bubbling
8	55.700	55.800	1.841	1.843	26.500	59.900	59.800	33.400	33.300						Bubbling
9	59.800	59.800	1.908	1.908	28.200	60.600	61.700	32.400	33.500	1.200	1.170	1.230	0.990	1.148	Slugging
10	64.500	65.000	1.981	1.989	30.600	63.000	63.200	32.400	32.600	1.490	1.480	1.350	1.580	1.475	Slugging
11	69.800	69.900	2.061	2.063	32.600	65.600	65.600	33.000	33.000	1.600	1.660	1.650	1.510	1.605	Slugging
12	75.300	75.200	2.141	2.140	34.700	68.600	68.200	33.900	33.500	1.730	1.780	1.710	1.830	1.763	Slugging
13	85.200	85.800	2.277	2.285	39.200	73.800	74.000	34.600	34.800	1.790	1.840	1.730	1.730	1.773	Slugging
14	95.300	94.900	2.409	2.404	43.500	78.800	78.400	35.300	34.900	2.010	2.050	1.860	1.790	1.928	Slugging
15	105.200	105.500	2.531	2.534	47.900	83.800	83.800	35.900	35.900	2.300	1.990	2.030	2.100	2.105	Slugging
16	114.900	115.200	2.645	2.648	52.200	88.300	88.900	36.100	36.700	2.280	2.200	2.230	2.280	2.248	Slugging
17	124.700	124.500	2.755	2.753	56.300	93.000	92.800	36.700	36.500	2.270	2.510	2.310	2.400	2.373	Slugging
18	135.300	135.300	2.870	2.870	60.500	97.200	97.400	36.700	36.900						Swirling
19	144.900	145.300	2.970	2.974	64.900	101.700	102.300	36.800	37.400						Swirling
20	165.300	-	3.172	-	73.100	111.700	-	38.600	-						Swirling

Shape: Cylindrical Size: L/D=4.10 Mass: 2000g Inclination: 10deg Overlap: 18deg

Data No.	ΔP across orifice		Superfical Velocity		ΔP across distributor	ΔP across distributor with particle		ΔP across bed		Slugging Time					Observation
	Forward	Reverse	Forward	Reverse		Forward	Reverse	Forward	Reverse	T1	T2	T3	T4	Tavg	
	mmH_2O	mmH_2O	m/sec	m/sec	mmH_2O	mmH_2O	mmH_2O	mmH_2O	mmH_2O	s	s	s	s	s	
1	30.000	29.400	1.351	1.338	15.100	54.400	45.200	39.300	30.100						Fluidization
2	32.900	32.900	1.415	1.415	16.700	57.800	48.900	41.100	32.200						Channeling
3	38.300	38.300	1.527	1.527	19.000	59.300	55.600	40.300	36.600						Channeling
4	42.400	42.500	1.607	1.608	20.700	63.000	60.300	42.300	39.600						Channeling
5	46.000	45.500	1.673	1.664	22.300	64.900	63.500	42.600	41.200						Channeling
6	49.600	49.900	1.738	1.743	24.000	66.500	66.100	42.500	42.100						Bubbling
7	55.000	55.300	1.830	1.835	26.500	69.500	69.500	43.000	43.000						Bubbling
8	59.400	60.200	1.902	1.914	28.200	71.600	71.700	43.400	43.500						Bubbling
9	64.800	65.500	1.986	1.997	30.600	73.900	74.200	43.300	43.600						Bubbling
10	69.500	69.500	2.057	2.057	32.600	76.400	76.200	43.800	43.600						Bubbling
11	74.500	74.600	2.130	2.131	34.700	78.900	79.400	44.200	44.700	Minor Slugging					Bubbling
12	84.700	85.300	2.271	2.279	39.200	84.200	84.500	45.000	45.300	1.270	1.330	1.370	1.270	1.310	Slugging
13	95.100	94.800	2.406	2.402	43.500	89.200	89.300	45.700	45.800	1.760	1.550	1.740	1.650	1.675	Slugging
14	105.200	105.400	2.531	2.533	47.900	94.100	94.300	46.200	46.400	1.730	1.660	1.710	1.760	1.715	Slugging
15	114.700	114.800	2.642	2.644	52.200	98.300	98.800	46.100	46.600	1.730	1.870	1.760	1.850	1.803	Slugging
16	125.400	124.900	2.763	2.757	56.300	102.800	103.100	46.500	46.800	2.150	1.890	1.840	2.020	1.975	Slugging
17	135.600	135.000	2.873	2.867	60.500	107.800	107.900	47.300	47.400	2.040	2.040	2.150	2.230	2.115	Slugging
18	144.600	144.600	2.967	2.967	64.900	111.600	111.600	46.700	46.700	2.160	2.170	2.220	2.080	2.158	Slugging
19	165.700	165.200	3.176	3.171	73.100	121.500	121.000	48.400	47.900						Swirling
20	185.100	-	3.357	-	82.000	130.300	-	48.300	-						Jumping

APPENDIX C: PROJECT RECOGNITIONS

ASME
SETTING THE STANDARD

Three Park Avenue
New York, NY
10016-5990 U.S.A.

tel 1.212.591.7000
fax 1.212.591.7674
www.asme.org

06/13/2012

Mr. Jia Jun Goo

Universiti
Teknologi
PETRONAS
Bandar Seri
Iskandar.
Tronoh, 31750
Malaysia

Dear Mr. Jia Jun Goo:

It is my pleasure to invite you to ASME 2012 International Mechanical Engineering Congress & Exposition (IMECE), which is being held from 11/09/2012 to 11/15/2012 in Houston, TX, USA.

You will be presenting the paper(s), Paper #:IMECE2012-93262 "Hydrodynamic Characterization of a Swirling Fluidized Bed (SFB)"

ASME is the premier organization for the promotion of the art, science, and practice of mechanical engineering throughout the world. Our mission is to promote and enhance the technical competency and professional well-being of our members, and through quality programs and activities in mechanical engineering better enable its practitioners to contribute to the well-being of humankind.

You are expected to undertake all expenses.

Victoria Chillemi,
Director, Enterprise Support
Tel: +1 (973)882-1170
Fax: +1 (973)882-1717
E-mail: chillemiv@asme.org

Figure 7.2: Technical paper accepted by ASME Congress 2012

UNIVERSITI TUN HUSSEIN ONN MALAYSIA

FAKULTI KEJURUTERAAN MEKANIKAL DAN PEMBUATAN
Tel : 07-4537701/7703/7707 Faks : 07-4536080

Rujukan Kami (Our Ref) : UTHM/FKMP/100-36/5/1 Jld 2(215)
Rujukan Tuan (Your Ref) :
Tarikh : 9 July 2012

Goo Jia Jun, Vijay R. Raghavan and Chin Yee Sing
Hydrodynamic Study of Fluidization in Gas-Solid Swirling Bed.
goojiajun@gmail.com, vijay@oyl.com.my, chinyeesing@petronas.com.my

Dear Prof. /Dr. /Mr. /Mrs. /Miss/Ms.

STATUS OF FULL TECHNICAL PAPER SUBMITTED FOR 3rd INTERNATIONAL CONFERENCE ON MECHANICAL AND MANUFACTURING ENGINEERING 2012 (ICME2012)

Paper no.: ICME2012-ID-143
EARLY BIRD REGISTRATION

Thank you for your full technical paper submission and interest.

The ICME2012 Technical Review Committee has completed the review for your paper and suggested the following recommendations:

Status of technical paper

Accepted with revision	✓
Accepted	

Publication

Will be published in the Applied Mechanics and Materials Journal (ISSN 1660-9336)	✓

Figure 7.3: Technical paper accepted by ICME 2012

Effect of Particle Shape on Bed Pressure Drop in a Swirling Fluidized Bed

Venkiteswaran, V. K. and Goo, Jia Jun and Chin, Yee Sing and Sulaiman, S. A. and Raghavan, V. R. (2012) *Effect of Particle Shape on Bed Pressure Drop in a Swirling Fluidized Bed.* In: 3rd International Conference on Production, Energy and Reliability, 12-14 June 2012, Kuala Lumpur.

PDF
Restricted to Repository staff only
77Kb

Abstract

In fluidized bed processes, bed pressure drop is crucial as it determines the pumping power required. However, the physical parameters that influence the bed pressure drop are yet to be fully established. The present work studies the effect of particle shape on bed pressure drop in a swirling fluidized bed. The three different shapes of particle used in the work are; cylindrical, spherical and ellipsoidal, with different bed weights (0.5 kg, 0.75 kg and 1.0 kg). Blades with overlap angle of 9° and blade inclination of 10° were used in this experiment. The results showed an increase in the bed pressure drop with an increase in bed weight for all three particles regardless of shape. Spherical shaped particles were seen to have the highest pressure drop compared to the others due to a smaller exposed surface area.

Item Type:	Conference or Workshop Item (Paper)
Subjects:	T Technology > TJ Mechanical engineering and machinery
Departments / MOR / COE:	Departments > Mechanical Engineering Mission Oriented Research > Energy
ID Code:	7740
Deposited By:	Dr Ir Shaharin A Sulaiman
Deposited On:	22 Jun 2012 15:05
Last Modified:	22 Jun 2012 15:05

Repository Staff Only: item control page

Figure: Technical paper published in ICPER 2012
Retrieved August 02, 2012 from eprints.utp.edu.my.

UNIVERSITI TEKNOLOGI PETRONAS

30

SCIENCE&ENGINEERING DESIGN EXHIBITION

Certificate of Participation

This certificate is awarded to

GOO JIA JUN
880520-56-5987

in recognition of his contribution as

Participant of
Final Year Project

"Gold"

in the 30th edition of

SCIENCE AND ENGINEERING DESIGN EXHIBITION
UNIVERSITI TEKNOLOGI PETRONAS

held on
8 - 9 August 2012

Dr. Dennis Ling Chuan Ching
Chairman
30th Science and Engineering Design Exhibition

Prof. Ir. Dr. Ahmad Fadzil B. Mohamad Hani
Deputy Vice Chancellor, Academic
Universiti Teknologi PETRONAS

SCIENCE AND ENGINEERING DESIGN EXHIBITION • SEDEX PORTAL TO THE FUTURE • UNIVERSITI TEKNOLOGI PETRONAS

Figure 7.5 : Gold medal award in SEDEX 30th, 2012

Certificate for Oral Presentation

Paper Title: Experimental Study on the Hydrodynamics of Swirling Fluidized Bed (T0124)

This is to certify that Jia Jun Goo from Universiti Teknologi PETRONAS, Malaysia has attended, and delivered an oral presentation in the 2012 International Conference on Mechanical and Electrical Technology (ICMET 2012) held in Kuala Lumpur, Malaysia during July 24-26, 2012.

Conference Committee
ICMET 2012

Figure 7.6: Technical paper published in ICMET 2012